

Review

Electrolyte Additive Strategies for Suppression of Zinc Dendrites in Aqueous Zinc-Ion Batteries

Chongyuan Zhai ¹, Dandi Zhao ¹, Yapeng He ^{1,2,3,*} , Hui Huang ^{1,2,3}, Buming Chen ^{1,2,3}, Xue Wang ^{4,*} and Zhongcheng Guo ^{1,2,3}

¹ Faculty of Metallurgical and Energy Engineering, Kunming University of Science and Technology, Kunming 650093, China

² Metallurgical Electrode Material Engineering Technology Research Center of Yunnan Province, Kunming 650106, China

³ Kunming Hendera Technology Co., Ltd., Kunming 650106, China

⁴ College of Chemistry and Chemical Engineering, Yunnan Normal University, Kunming 650500, China

* Correspondence: heyapeng@kmust.edu.cn (Y.H.); xwang@ynnu.edu.cn (X.W.)

Abstract: Aqueous zinc-ion batteries (ZIBs) with metal zinc as the anode possess the features of safety, environmental friendliness, and high specific capacity, which have attracted a great deal of attention in the past few years. The accompanying zinc dendrites are an important problem that endangers the battery performance. Therefore, the extensive research on the suppression strategies of Zn dendrites reflects a positive effect on improving the performance of ZIBs. In particular, the electrolyte additives (EAs) approach is considered a simple, reliable, and low-cost strategy to address the zinc dendritic issues and can inhibit or alleviate the growth of zinc dendrites while facilitating the amelioration of adverse reactions. In this review, the principles and processes of zinc dendrites, corrosion passivation, and hydrogen evolution side reactions on zinc anodes of ZIBs are firstly categorized. Then, the mitigation and inhibition of zinc dendrites and side reactions via different kinds of EAs are elaborated according to the regulation strategies of EAs, which provides an overview of the research on EAs conducted in recent years and proposed strategies to solve zinc dendrites and other problems. Finally, a reasonable outlook on the future improvement and development of EAs for ZIBs is described, which could provide some guidance for the evolution and design of EAs in the future.

Keywords: aqueous zinc-ion battery; Zn anode; zinc dendrites; electrolyte additives; regulation mechanism



Citation: Zhai, C.; Zhao, D.; He, Y.; Huang, H.; Chen, B.; Wang, X.; Guo, Z. Electrolyte Additive Strategies for Suppression of Zinc Dendrites in Aqueous Zinc-Ion Batteries. *Batteries* **2022**, *8*, 153. <https://doi.org/10.3390/batteries8100153>

Academic Editors: Guojin Liang and Funian Mo

Received: 29 August 2022

Accepted: 27 September 2022

Published: 2 October 2022

Publisher's Note: MDPI stays neutral with regard to jurisdictional claims in published maps and institutional affiliations.



Copyright: © 2022 by the authors. Licensee MDPI, Basel, Switzerland. This article is an open access article distributed under the terms and conditions of the Creative Commons Attribution (CC BY) license (<https://creativecommons.org/licenses/by/4.0/>).

1. Introduction

With the progression and development of human society, the accelerated depletion of traditional energy sources and environmental pollution have become the focus of extensive concern. Thus, the exploration of economic, environment friendly and reliable renewable energy sources will be the prevailing trend. In particular, the employment of solar, wind, and hydropower as the mainstream of new energy development has become a credible source of energy supply [1–3]. Nevertheless, due to the space–time and geographical conditions, the deployment of advanced energy storage devices is profoundly meaningful for improving the storage and release of energy, which holds great promise for development in all types of energy storage applications. For a long time, Li-ion batteries (LIBs) have emerged as an essential energy storage device for various electrical devices due to their favorable electrochemical properties, including high capacity and superior endurance [4–6]. However, there are critical limiting issues facing LIBs, such as high price, low abundance, relatively low power density and flammability, which remarkably define their global characteristics and severely hinder their wide-spread applications [7–9]. Therefore, the current field of electrochemical energy storage still lacks a suitable battery system possessing large

energy density, high security, environmental friendliness, and low cost to meet the practical requirements of large-scale energy conservation.

Compared to alkali metals, such as lithium, sodium, and potassium, metal zinc (Zn) exhibits the features of low cost and abundant reserves, where the small ionic radius (0.74 Å) of Zn facilitates the migration/storage during the charging/discharging process. Meanwhile, metal Zn also demonstrates the advantages of low redox potential (−0.76 V vs. SHE), high specific capacity (820 mAh g^{−1}), and non-toxic reliable aqueous electrolyte [10,11]. In addition, metal Zn also exhibits high ionic conductivity and reversibility in aqueous electrolyte that is more stable than alkaline electrolytes, which makes ZIBs promising as a new class of electrochemical energy storage devices. However, the critical issues, including dendrites growth, corrosion passivation, and hydrogen evolution parasitic reactions (HER) on zinc anodes, currently prominently plague the lifespan and performance of ZIBs. Essentially, uneven electric field strength and ion concentration on zinc anode result into the disorderly nucleation and growth of metal zinc, where the random growth of zinc dendrites will penetrate the separator and induce the short circuiting of ZIBs, greatly shortening the life of the battery [12]. Additionally, the hydrogen evolution, corrosion, and passivation reactions that occur on zinc anodes cause massive depletion of cations in the electrolyte and generate dead zinc adhering to the anode surface, resulting in increased electrode polarization and reduced electrochemical performance. Therefore, zinc dendrites, corrosion, and HER are considered the major challenges that need to be addressed in ZIBs [13–15].

So far, many advanced foresighted strategies have been proposed to tackle the issues of zinc dendrites and surface side reactions, which mainly consist of constructing ion coordination layers on the zinc anodes [16], establishing fast stereoscopic channels for ions to achieve uniform ion distribution [17,18], building charge uniform distribution coatings [19,20], designing stereoscopic structures [21,22], optimizing electrolyte additives [23–26], etc., as presented in Figure 1. Among above multidimensional approaches, the coating and surface structural modification of the anode commonly display the complicated process of the materials preparation and high cost, and the prospect of the future application of the approaches is still not clear. In contrast, the solution employing the EAs with different properties is effective and simple, which has been extensively explored in last few years. As a result, EAs have already been successfully employed as a facile technique in many types of batteries, such as LIBs and ZIBs [27–30]. In terms of the detailed effectiveness, the introduction of EAs will increase the anode stability [31], suppress the generation of dendrites, improve the coulomb efficiency [32], reinforce the extreme adaptability over a wide temperature range [33], etc. From these aspects, it is concluded that EAs are widely utilized, and the research on EAs is extremely imperative and prospective.

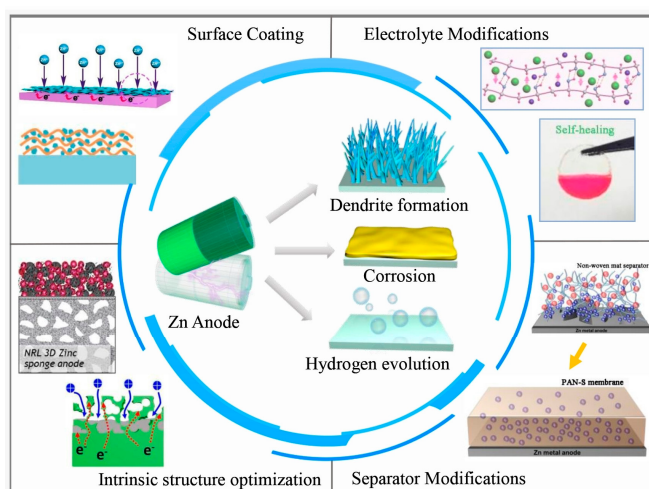


Figure 1. Schematic of unfavorable effects and stabilization strategies for Zn anode. Reproduced with permissions from Ref. [15]. Copyright © 2022 WILEY-VCH.

Commonly, different types of additives exhibit various effects on the electrochemical behaviors of the ZIBs. The main problems solved by the EAs would also be also different. Hence, it is essential to summarize the classification and detailed role of various types of EAs. It is also important to grasp the action mechanism and the effect of different EAs for improving the battery performance and conducting subsequent research.

2. Surface Reactions on Zn Anode

The operation mechanism of ZIBs is essentially attributed to Zn^{2+}/Zn electrochemical redox; therefore, the reversibility of the deposition/stripping behavior is incredibly valuable to achieve stable and long operation features of ZIBs [34,35]. It is well known that the electrolyte system dominates the electrochemical energy storage system, and there are two main electrolyte systems for ZIBs, alkaline and weakly acidic system. The reactions carried out at the zinc anode in above two environments are different. In general, Zn^{2+} ions are coordinated in the electrolyte with six H_2O molecules in the solvated structure of $(Zn(H_2O)_6)^{2+}$, as described in Figure 2a. The solvated active water molecule is easily decomposed into H^+ and OH^- at the interface between the anode and electrolyte. H^+ gradually accumulates on the anode to obtain electrons and generates H_2 , while OH^- is transformed into a by-product. The solvation effect induces the charge transfer through the O-H bond of the solvated Zn^{2+} , weakening the hydrogen bond created by the movement of electrons from the bonded molecular orbital of the ligand water to the unoccupied Zn^{2+} orbital [36]. In alkaline electrolytes, the O-H bonds in the solvated $(Zn(H_2O)_6)^{2+}$ are prone to be adsorbed by the more strongly O-H bonds in the electrolyte, forming the $Zn(OH)_2$ complexes. By further deprotonation to form the $Zn(OH)_4^{2-}$, the severe concentrated polarization promotes the inhomogeneous distribution of zincate during the consumption of the zincate in the electrolyte around the anode, which is then converted into passivated zinc oxide deposits [15,37]. The detailed reaction formula is presented as follows.

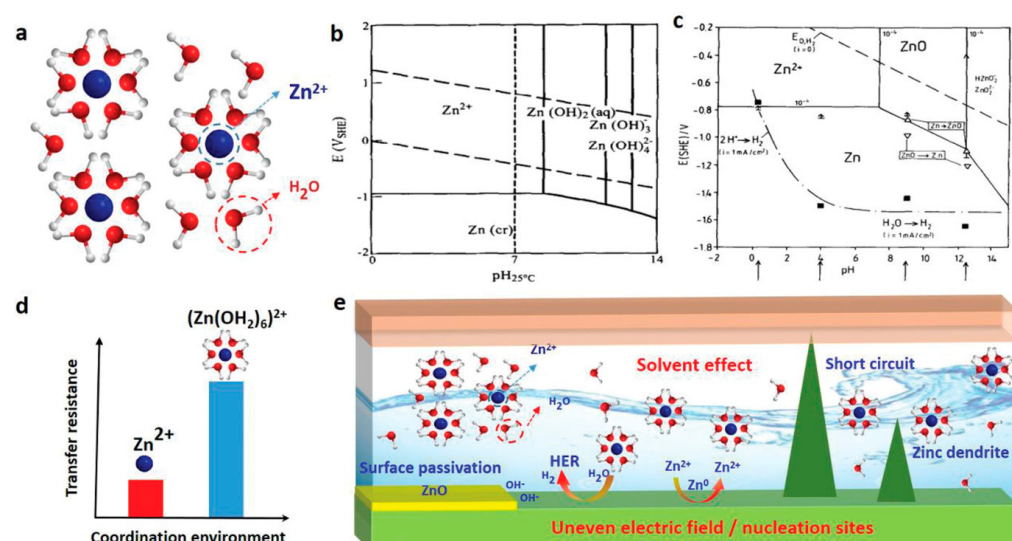
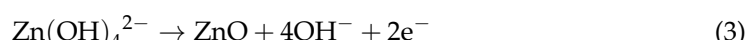
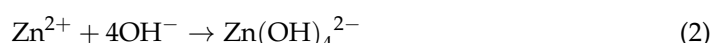


Figure 2. (a) The coordination environment of Zn^{2+} in aqueous electrolyte. (b) Pourbaix diagram of the Zn/H_2O system. (c) Pourbaix diagram of the Zn/H_2O system including HER overpotential changes. (d) Comparison of transfer resistance with different coordination environments. (e) Schematic diagram of the impact factors on the decay of zinc anode performance. Reproduced with permissions from Ref. [38]. Copyright © 2020 WILEY-VCH.

As for the weakly acidic electrolyte system, the weakly acidic medium could protect the presence of $(\text{Zn}(\text{H}_2\text{O})_6)^{2+}$. The local alkaline environment can force the presence of $\text{Zn}(\text{OH})_4^{2-}$, which subsequently translates into the passivated electrochemically ZnO precipitates, thus significantly increasing the interface resistance and failing the battery property [38]. On the contrary, the reversible adsorption and desorption of zinc ions in weakly acidic environment reduces the effect of side reactions on the electrochemical performances [39]. As discussed above, the electrolyte system is the core operation area of ZIBs. Although the extent of side reactions in the two electrolyte systems is slightly different, the mechanisms and suffered hazards, such as dendrite growth, corrosion, HER and by-products on the anode surface, are generally similar in the different electrolytes. That is, zinc dendrites, corrosion, and HER are considered the major challenges that need to be addressed in ZIB.

2.1. Zinc Dendrites

Like other metal ion batteries, zinc dendrites are one of the most important problems plaguing the development of ZIBs and have received widespread attentions. The condition of the electrode interface primarily determines the generation of zinc dendrites, and the detailed parameters consist of electric field distribution, ion concentration distribution, and nucleation location of the deposited zinc. General speaking, there are two main stages during the formation of zinc dendrites, which are nucleation and growth stages, respectively. Most of the current ZIBs systems employ zinc foil as the anode to provide zinc ions and act as the collector, where the surface is not, in fact, flat. In the early stage of the nucleation process, zinc ions are adsorbed on the anode by the electric field force [40]. During the charging process, the nucleation overpotential, which is defined as the difference between the tip potential and subsequent stable potential and refers to the thermodynamic cost of forming a critical atom cluster, increases as the zinc ions continue to react with the electrons due to the decreased migration ability of zinc ions and high mass-transfer overpotential based on the thermodynamic considerations [41]. When the overpotential exceeds the nucleation barrier, metal zinc is deposited on the anode surface and diffuses freely, forming an initial zinc nucleus by aggregating with other atoms [42,43]. As the zinc nuclei accumulate into small bumps, the tips of the bumps produce a “tip discharge” effect [44]. That is, great curvature of the tip of the bump and high surface charge density attract zinc ions to deposit at the tip of the bump and reinforce the formation of dendrites. As the loose dendrites break and detach from the collector, “dead zinc” will be formed, which would greatly reduce the coulombic efficiency and capacity of ZIBs, making the life of the battery significantly reduced. Even worse, as the cycle progresses, the growth of dendrites will penetrate the separator and make the Zn anode contact with the cathode, causing a short-circuit of the battery [45].

Although the dendrites problem on metal zinc anodes has been widely recognized by the scientific community, there is still a lack of a complete theoretical system to explain the formation mechanism of zinc dendrite in the electrolytes. According to the basic principles of electrochemistry, it is generally believed that the zinc dendrite consists of three main series of processes, namely mass transfer, charge transfer, and zinc electrocrystallization. The distributed deposition of zinc and suppression of zinc dendrites are beneficial to the cycling stability and high current efficiency of aqueous ZIBs. For a long time, the extensively utilized LIBs have been plagued by the dendritic problems [46,47]. In recent years, the dendrite growth of the anode has also been a difficult challenge for the rapidly development of the ZIBs.

The excessive and disorderly growth of dendrites brings some incalculable damages, which severely disrupt the normal operation and lifetime of ZIBs [48]. First, as the zinc dendrites grow, the contact zone between the zinc anode and electrolyte increases, which exacerbates a series of harmful adverse reactions. Secondly, the zinc dendrites lead to the loose structure and rough surface, which will enhance the specific surface area of the anode and further aggravate the surface parasitic reactions, including corrosion and

HER. Additionally, some by-products will be formed via the chemical interaction between the electrolyte and dendrites after the disrupted dendrites enter into the electrolyte. The by-product will also adsorb on the electrode materials, increasing the impedance of the system and further reducing the coulombic efficiency. Therefore, uniform electric field distribution on the metal Zn anode or homogenized deposition of zinc ions during cycling is the key to address the zinc dendrite issues [10]. Thirdly, due to the tip effect, dendrites are continuously gathered in the tip bumps, resulting in the extension of the length of dendrites, which will then penetrate the separator and contact with the cathode, leading to short circuit and damage between anode and cathode, significantly reducing the battery life. Therefore, it is important to study the internal factors affecting zinc dendrites and propose countermeasures to tackle the dendrite problem in ZIBs.

2.2. Hydrogen Evolution Parasitic Reaction

In addition to the growth of Zn dendrites, another major side reaction occurring at the zinc anode is the hydrogen evolution parasitic reaction (HER). Theoretically, HER could occur over the entire pH range between resting and working processes, as displayed in Figure 2c. Despite the fact $E^\theta_{H+} > E^\theta_{Zn^{2+}}$ [10], metal zinc deposits preferentially over hydrogen gas practically due to sluggish hydrogen evolution kinetics, high overpotential, and low H^+ activity [15]. However, at the contact position between the electrolyte and zinc anode, HER prefers to be occurred on Zn anode, where the hydrogen evolution process is affected by various factors, such as temperature, applied current, electrolyte concentration, etc. [49] As mentioned in the previous section, the inhomogeneous ion concentration distribution caused by the formation of zinc dendrites will also affect the active sites of HER, which are also more likely to proceed at high polarization potentials. On the other hand, HER, as an irreversible side reaction, competes with the reversible zinc deposition reaction, leading to irreversible loss of electrolyte and zinc anode, which reduces the coulomb efficiency of the ZIBs. At the same time, the hydrogen released from the hydrogen evolution reaction collects inside the battery, causing bulging and even explosion of the cell.

2.3. Corrosion Passivation

The primary categories of the corrosion of Zn anode in electrolytes are chemical and electrochemical corrossions. Chemical corrosion involves the spontaneous reaction of zinc with water in the electrolyte to yield ZnO and H_2 , which further promotes side reactions by roughening the anode surface. The ZnO by-products from the corrosion increase the internal resistance of ZIBs, passivate the anode, and eventually lead to capacity decay. Electrochemical corrosion behavior is regarded as the main process of surface passivation, which includes the generation of Zn dendrite shedding and irreversible by-products. Theoretically, the corrosion behaviors of zinc anode are inextricably linked with the hydrogen evolution, where the electrochemical corrosion is also a major challenge of ZIBs. Commonly, zinc metal undergoes a relatively long corrosion process in the neutral solution environment, but the weakly acidic electrolyte system of ZIBs will speed up the process. When the zinc anode is immersed in the weakly acidic $ZnSO_4$ electrolyte of ZIBs, regular hexagonal $Zn_4(OH)_6SO_4 \cdot xH_2O$ flake by-products are generated [50], the formation of which inescapably consumes reactive Zn^{2+} and electrolyte, leading to a certain degree of capacity decay. In addition, the insoluble by-products adhere to the electrode surface, which block some reactive nucleation sites and form coarse protrusions on the zinc anode, leading to a non-ideal surface and promoting the production of zinc dendrites. Due to the poor electrical conductivity, the formed by-products also increase the charge transfer impedance and mitigate the electron and ion transport at the anode, resulting into the anode passivation, as displayed in Figure 2e. More importantly, these by-products do not prevent further corrosion after covering the zinc anode. As a result, the zinc metal and electrolyte stay in a constant depletion state during the cycling, resulting in lower coulombic efficiency, higher charge transfer resistance, and shorter cell life [51].

The three main problems that exist on the zinc anode surface are mutually reinforcing and interactive, where the zinc dendrites are considered the origin of many undesirable reactions. The produced loose and porous zinc dendrites accelerate HER and corrosion kinetics. Moreover, the adhesion of H_2 bubbles evolved on the anode hinders the zinc nucleation, leading to the increased overpotential and undulated zinc deposition. Meanwhile, the accumulation of OH^- generated by HER expedites the corrosion process, and the corrosion-induced roughness of the zinc surface may further exacerbate the production of dendrites. The large curvature and irregular by-product passivation layer also increase the contact area and accelerate HER.

Therefore, optimizing the electrolyte system to restrain the disorderly growth of zinc dendrites and improve surface structure of the anode are favorable to suppress the occurrence of parasitic reactions and optimize the performances of ZIBs. As for aqueous ZIBs, the EA approach is regarded as an appropriate option to realize a dendrite-free zinc anode.

3. Optimization of the Electrolytes

The aqueous electrolyte system of ZIBs demonstrates the advantages of low toxicity, safety, and high ionic conductivity, rendering it a favorable target for many researchers. Various types of zinc salts including $ZnSO_4$, $ZnCl_2$, $Zn(CH_3COO)_2$, $Zn(ClO_4)_2$, $Zn(CF_3SO_3)_2$, etc., have been developed as solution system in ZIBs. However, in the practical application of aqueous electrolyte system, the relatively low concentration (normally below 2 M) solution system leads to severe zinc dendrites, side reactions, and a narrow electrochemical stability window, which restricts the further wide application of aqueous ZIBs [52]. The coordination environment of zinc ions usually depends on the composition of the electrolyte, namely, the specific salt or solvent. Based on this, highly concentrated electrolytes are particularly suitable as an alternative to regulate the zinc ion environment based on the molecular level. To improve the stability of zinc anodes and suppress the generation of zinc dendrites, the researchers borrow from the water-in-salt electrolyte (WISE) system in previous electrocatalysis and battery fields, in which the salt mass and volume are higher than the solvent by modifying the salt-to-water ratio in the electrolyte. As a result, a sufficient solubility of salt enhances the ionic conductivity of the electrolyte and solves the problems of zinc dendrites and side reactions, thus improving the electrochemical performance [53]. In this way, the increase in salt concentration changes the coordination configuration of Zn^{2+} ions, which are well surrounded by different salt anions instead of H_2O molecules, avoiding the direct contact of H_2O with the metal Zn anode. Moreover, the H_2O/H_2 equilibrium potential decreases with decreasing H_2O concentration (i.e., increasing salt concentration in the electrolyte), further limiting the formation of H_2 . Due to the absence of OH^- generation, the inactive $Zn(OH)_2$ and ZnO on the metallic zinc surface can also be suppressed, greatly improving the Coulomb efficiency and reducing the interfacial resistance. The WISE system has been extensively investigated by increasing the concentration of the original electrolyte or using a combination of highly concentrated ionic salts to lower the content of free water in the electrolyte, achieving an ordinated deposition of Zn^{2+} and a significant improvement in the lifetime and cycling performance of ZIBs.

As a sample, Wang et al. [54] employed 3 M $ZnSO_4$, 3 M $ZnCl_2$, and 30 M $ZnCl_2$ as the electrolytes for ZIBs, respectively. The WISE system constructed by 30 M $ZnCl_2$ significantly improved the rate performance of ZIBs, while the zinc dendrites and side reaction problems at the anode were apparently suppressed. The advantages and excellent electrochemical performance of the explored WISE system could be attributed to the large ionic conductivity of WISE, where 73% capacity retention was achieved after 100 cycles at a high current density of 100 mA g^{-1} , compared to the corresponding 14% and 18% for 3 M $ZnSO_4$ and 3 M $ZnCl_2$. The relevant results revealed that Zn^{2+} in 3 M $ZnSO_4$ accumulated directly on the anode to form dendrites, where irreversible $Zn_4SO_4(OH)_6 \cdot H_2O$ was generated, increasing the contact area where corrosion and HER side reactions occurred. Due to the etching of the layered cathodic MoO_3 , Zn^{2+} was irreversibly embedded in MoO_3 cathode,

and the detached Mo(VI, V) from the cathode was reduced to form MoO_x on the anode surface, which increases the charge impedance and leads to a decrease in life. On the contrary, in the WISE system, the Zn²⁺ generated on the anode surface was uniformly distributed, where WISE inhibited the cathodic dissolution to reduce the deposition of MoO_x and make the shape regular. More importantly, a high concentration of WISE reduced the amount of free water, and the resulting Zn₅(OH)₈Cl₂·H₂O was reversible and lowered the HER side reactions, as shown in Figure 3. The low-cost and safe WISE system constructed with ZnCl₂ provided a new idea to suppress Zn dendrites and improve the electrochemical stability.

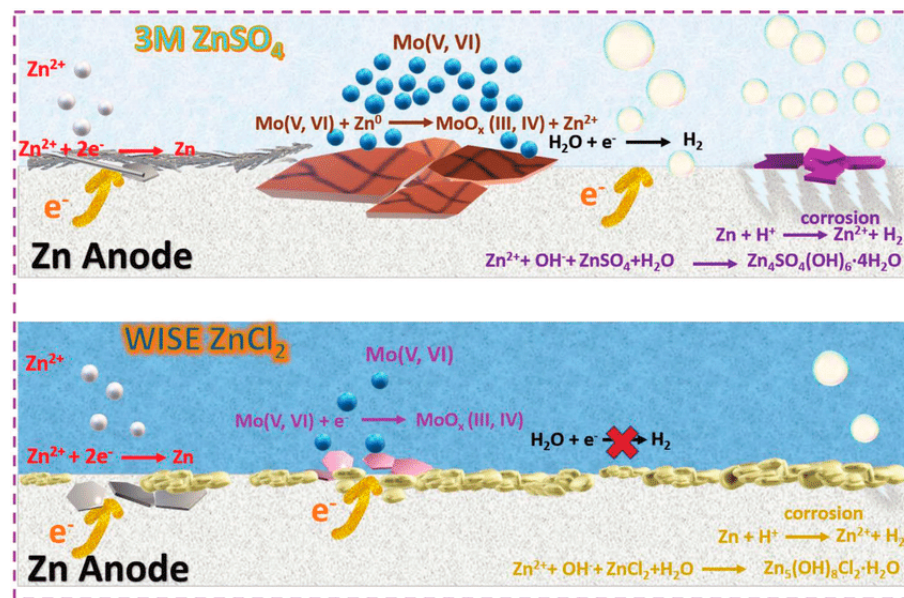


Figure 3. Schematic showing the plausible reaction mechanisms at both MoO₃ cathode and Zn anode in the 3 M ZnSO₄ and 30 M ZnCl₂ WISE. Reproduced with permissions from Ref. [54]. Copyright © 2021 WILEY-VCH.

In addition to directly increasing the concentration of zinc salts, the addition of other salts could also change the structure of hydrated Zn²⁺ ions. For instance, Zhang et al. [55] constructed a WISE system using 21 M LiTFSI + 3 M Zn(TfO)₂ to maximize the salt content in the electrolyte by increasing the concentration of LiTFSI. The electrochemical stability window of the anode (2.6 V vs. Zn²⁺/Zn) was significantly higher than that of the 3 M Zn(TfO)₂, where the high salt concentration reduced the proportion of free water in the electrolyte, increased the ionic conductivity, and expanded the electrochemical stability window of the anode. After 400 stripping/plating cycles, the surface of the anode showed a homogeneous and dense morphology without the generation of zinc dendrites, and WISE system exhibited an effective inhibition of zinc dendrites, thus improving the reversibility of the anode. The constructed Zn-ion battery with the reversible anion intercalation chemistry in graphite cathode exhibited good reversible cycling performance with a Coulombic efficiency of 95%, which was comparable to that of organic electrolyte-based dual-ion batteries, as presented in Figure 4. In short, the WISE system provides wide operating voltage and unprecedented cycling stability, providing fresh possibilities for the exploitation of high-voltage rechargeable aqueous batteries.

On the other hand, WISE systems could also employ high salt concentrations to decrease the activity of free water in the electrolyte and change its solvation structure by coordination with Zn²⁺ to achieve a controlled regulation of the unfavorable reaction. Bizualem [56] reported a concentrated aqueous electrolyte system (CZSAE, 4.2 M ZnSO₄ + 0.1 M MnSO₄), where the combination of electrolytes with lower concentrations was utilized to produce an electrolyte that effectively improves the cyclic stability of zinc

anodes. Drawing on the Raman spectroscopic techniques, X-ray absorption spectroscopy, and molecular dynamics in aqueous solution presented in Figure 5, it could be noticed that in the low concentrated ZnSO_4 aqueous electrolyte (LZSAE) containing 2 M ZnSO_4 + 0.1 M MnSO_4 , Zn^{2+} is surrounded by six free water molecules in coordination. As for CZSAE, due to the change of salt concentration in the electrolyte, a high concentration of SO_4^{2-} can be coordinated with Zn^{2+} , thus changing the solvated structure of Zn^{2+} and reducing the generation of side reactions. Under 0.2 mA cm⁻², the initial morphology of anodic zinc deposition in LZSAE showed obvious uniformity, while a non-uniform, dust-like bump was formed after 10 cycles, indicating the production and growth of zinc dendrites. On the other hand, the zinc deposition on the anodic surface was more uniform and regular in CZSAE, forming a stable zinc layer. As a result, a highly stable and reversible Zn/MnO_2 cell with 88.37% capacity retention was obtained after 1200 cycles at 938 mA g⁻¹ with dendritic-free homogeneous Zn plating.

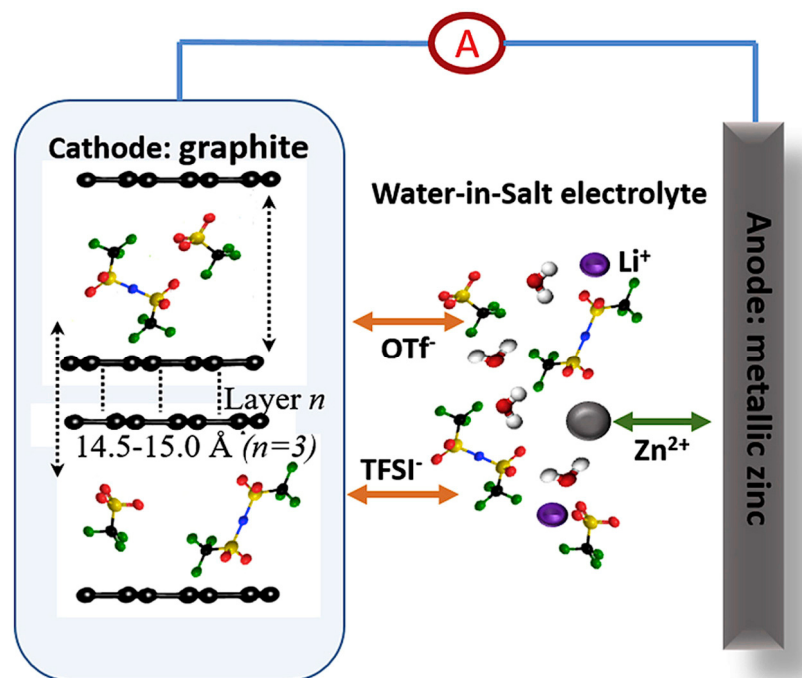


Figure 4. Schematic of TFSI^- and TfO^- anions intercalated into graphite with a repeating distance ranging from 14.5 nm to 15.0 Å in aqueous dual-ion battery, where positive electrode operates with the anion intercalation and the negative feature zinc plating/stripping. Reproduced with permissions from Ref. [55]. Copyright © 2020 Elsevier Ltd.

The exploration of the simple WISE strategy achieved the inhibition of zinc dendrite and reduced the occurrence of parasitic reactions under high-concentration salt conditions, which brought new ideas for the construction of stable zinc anodes and long cycle life of ZIBs. Although highly concentrated electrolytes and anhydrous electrolytes could significantly expand the electrochemical stability window, the large-scale application of these strategies is hindered by the high cost of conventional aqueous electrolytes.

3.1. Electrolyte Additives for Zinc Dendrites

The employment of the typical electrolytes containing functional additives to endow them significant crystal direction and surface textrization could prominently suppress zinc dendrites and thus refine the reversibility and stability of zinc anodes, such as metal salts, amino acids, surfactants, organic ethers, alcohols, ionic liquids, etc. Numerous EAs that have been investigated recently can be broadly classified into the categories including ionic, organic, inorganic additives, etc. [25,52], which have played a key role in solving the zinc

dendrites problems, achieving significant results in protecting the anode and optimizing the overall battery performance [53,57–59].

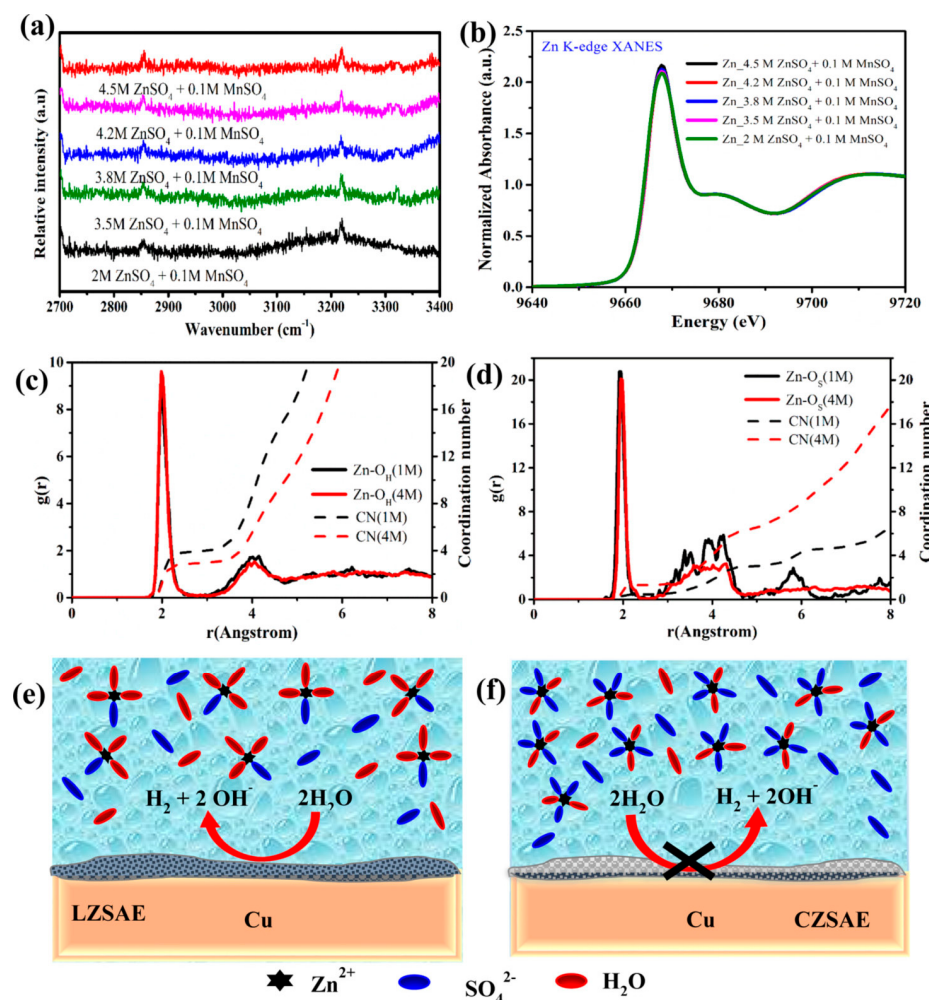


Figure 5. (a) Characteristic Raman spectra for different concentrations of zinc-salt electrolytes and (b) Zn K-edge XANES for different concentrations of zinc-salt electrolytes. RDFs (solid line), $g(r)$, and the corresponding integrals of CNs (dashed line), for (c) Zn-OH and (d) Zn-OS with salt concentration from 1 M (black) to 4 M (red) at 300 K, schematic representation for the passivation layer ($\text{Zn}_4(\text{OH})_6\text{SO}_4 \cdot x\text{H}_2\text{O}$) formation and solution structure during Zn plating in (e) LZSAE and (f) CZSAE systems. Reproduced with permissions from the Ref. [56]. Copyright © 2020 American Chemical Society.

3.2. Ionic Additives

Ionic additives are the simplest and most widely used among the types of electrolyte additives, which possess the features of simple preparation and abundant resources while exhibiting excellent performance. Ionic additives can not only modify the reaction mechanism and optimize the electrochemical performances of the cathode, but also increase the ionic conductivity of the electrolyte and regulate the dendrite production on zinc anode. Commonly, most of ionic additives are based on metal ions as the main additives, such as CuSO_4 , PbSO_4 , NiSO_4 [60], MgSO_4 [61], $\text{La}(\text{NO}_3)_3$ [62], and MnSO_4 [63], and organic cations [64,65], which could enhance the electrolyte ionic conductivity in solution and cooperate with zinc ions to achieve the controlled regulation of zinc dendrites and play a role in protecting the battery. The summary is displayed in Table 1.

Table 1. Ionic additives and effects in ZIBs.

Solution with Additives	Effects	Operation Parameters and Results	Ref.
1.25 M $(\text{NH}_4)_2\text{SO}_4$ + 2 M $\text{NH}_3 \cdot \text{H}_2\text{O}$ + 0.5 M ZnSO_4 + 1.67 mM PbSO_4	Inhibit zinc dendrites Improve formation of homogeneous zinc deposits	-	[60]
3 M ZnSO_4 + 2 M LiCl	Inhibit the formation of dendrites	0.2 mA cm^{-2} @ $0.0333 \text{ mAh cm}^{-2}$, 170 h	[66]
2 M ZnSO_4 + 0.1 M MnSO_4 + 0.5 M Na_2SO_4	Promote the uniform deposition Prevent further dissolution of Mn Improve the structure stability	0.2 mA cm^{-2} @ 0.2 mAh cm^{-2} , 300 h	[67]
2 M ZnSO_4 + 0.1 M MgSO_4	Inhibit the HER Enable uniform Zn nucleation/deposition Suppress the growth of Zn dendrites	1 mA cm^{-2} @ 0.25 mAh cm^{-2} , 600 h	[61]
2 M ZnSO_4 + 0.2 M MnSO_4 + 0.5% gelatin	Mitigate both dendrite growth and corrosion	0.25 mA cm^{-2} @ 0.05 mAh cm^{-2} , 500 h	[63]
1 M KCF_3SO_3 + 0.1 M $\text{Zn}(\text{CF}_3\text{SO}_3)_2$ + 0.1 M $\text{Al}(\text{CF}_3\text{SO}_3)_3$	Improve the reversibility Inhibit the formation of byproduct Improved the reversible deposition of zinc ions Weaken the EDL repulsive force	3 mA cm^{-2} , 1500 h	[68]
2 M ZnSO_4 + 8.5 mM $\text{La}(\text{NO}_3)_3$	Favor dense metallic zinc deposits Regulate the charge distribution Preferential adsorption of Ch^+ cations	1.0 mA cm^{-2} @ 1.0 mAh cm^{-2} , 1200 h	[62]
1 M ZnSO_4 with 4 M cholinium	Create “leveling effect” to homogenize Zn deposition Weaken water activity Promote the desolvation of hydrated Zn cations	1.0 mA cm^{-2} @ 1.0 mAh cm^{-2} , 2000 h	[64]
2 M ZnSO_4 + 0.2 M MnSO_4 + 25 mM KI + 25 mM I ₂	Extend the strip/plating stability of zinc Passivate zinc dendrite growth hotspots Reduce decomposition rate of H_2O and corrosion rate of Zn	1.75 mA cm^{-2} @ $0.585 \text{ mAh cm}^{-2}$, 1430 h	[69]

In previous studies, metallic Pb could be doped as an additive in the anode or electrolyte of alkaline batteries to reduce the deposition potential of Zn. The deposition of Pb occupies the active generation sites on Zn and promotes the uniform growth of metallic Zn [70]. Hoang et al. [24] investigated the effect of low concentration 1.67 mM Pb^{2+} on ZIBs and concluded that the addition of Pb^{2+} ions could effectively enhance the polarization effect, thus suppressing the growth of Zn dendrites. Specifically, Pb^{2+} ions promoted the fast response of current and high coverage in the electrode area, which substantially enhanced the utilization of the electrode surface and thus accelerated the balance of the deposited current. As a consequence, the zinc ions under the action of lead ions occupied more nucleation sites and the deposition morphology changed from dendritic to lamellar, which effectively protected the zinc anode from zinc dendrite growth. At the same time, the corrosion current on the zinc cathode was reduced by 20% by introducing the lead ion additive, which increased the service life of the ZIBs.

Metal cations with abundant natural resources are the most abundant part of ionic additives in ZIBs. For example, Xu et al. [67] reported a zinc/sodium manganese oxide (Zn/NMO) batteries constructed by Na_2SO_4 as an electrolyte additive in the $\text{ZnSO}_4 + \text{MnSO}_4$ system, which exhibited a high capacity of 367.5 mAh g^{-1} and ultra-long-term cycling stability with a capacity loss of only 0.007% after 10,000 cycles. The self-healing electrostatic shielding effect of Na^+ on the anode surface was elaborated, where the Na_2SO_4 additive in the ZnSO_4 electrolyte could mitigate Zn dendrites via changing the deposited model of Zn^{2+} ions, as depicted in Figure 6a. In the electrolyte without Na_2SO_4 , Zn^{2+} would be deposited on the anode surface at the tips of some protrusions, which exhibited a strong local electric field near the protruding tips, thus causing a large amount of Zn^{2+} to accumulate near the tips and progressively accumulate into lamellar Zn dendrites. As for the electrolyte containing Na^+ , when the voltage was higher than the reduction potential of Na^+ and lower than that of Zn^{2+} , Na^+ and Zn^{2+} ions were adsorbed on the anode surface simultaneously,

while Na^+ would preferentially accumulate near the tip and evolve into a local electrostatic protective layer, prompting the deposition of Zn^{2+} ions in the adjacent area around the tip and finally forming a smoothly deposited zinc coating, as described in Figure 6d–f. The assembled $\text{Zn} // \text{Zn}$ symmetrical cell with Na_2SO_4 additive can provide excellent cycling stability up to 300 h and low overpotential of 48.8 mV (Figure 6h), further illustrating the good electrochemical performance of introducing low reduction potential Na^+ .

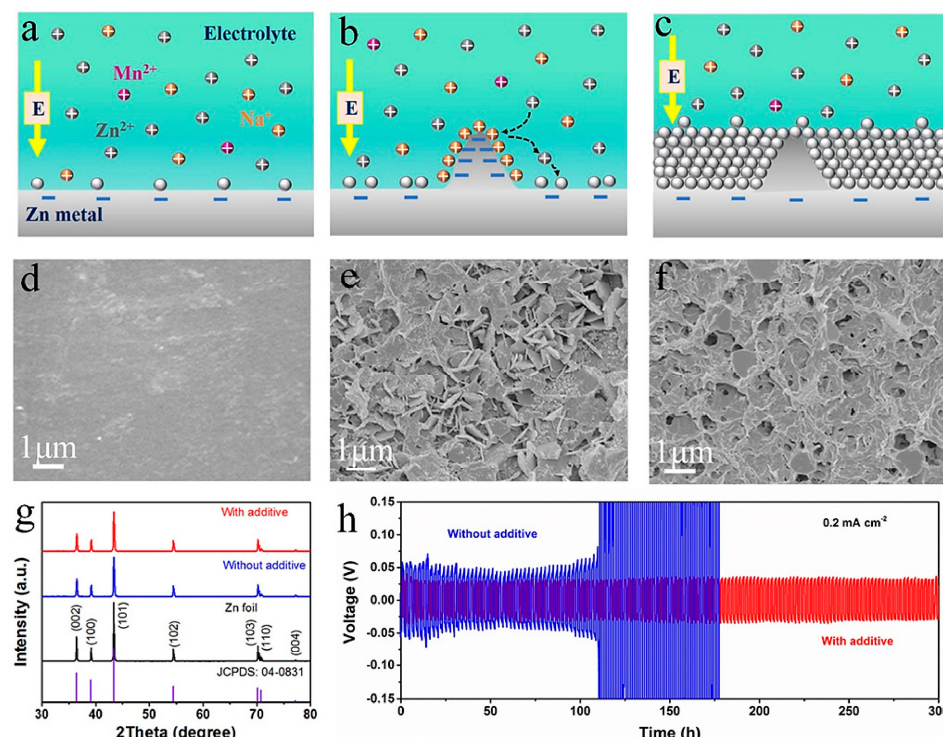


Figure 6. The influence of Na_2SO_4 additive on the metallic Zn anode. (a–c) Illustration of the Zn deposition process according to the electrostatic protection mechanism. (d) the SEM image of the commercial Zn surface before measurement. (e) the electrodeposited morphology of Zn surface after five CV tests in ZnSO_4 electrolytes without Na_2SO_4 additive. (f) the electrodeposited morphology of Zn surface after five CV tests in ZnSO_4 electrolytes with 0.5 M Na_2SO_4 additive. (g) The XRD patterns of fresh Zn foil and the electrodeposited Zn electrodes with/without Na_2SO_4 additive. (h) Polarization curves of $\text{Zn} // \text{Zn}$ symmetric batteries with/without Na_2SO_4 additive at a constant current density of 0.2 mA cm^{-2} . Reproduced with permissions from the Ref. [67]. Copyright © 2021 Elsevier Ltd.

Not coincidentally, Guo et al. [66] also noted the electrostatic shielding effect of metal ions with low reduction potential. In particular, LiCl was developed as an EA to investigate the synergistic effect of Li^+ and Cl^- in the inhibition of zinc dendrites. Similar to Na^+ , Li^+ could establish an electrostatic shielding protective oxide layer on the anode, and the anode surface in the electrolyte with LiCl addition was smooth, and the mossy surface of petal-like zinc dendrites did not appear. By comparing Cl^- with NO_3^- and SO_4^{2-} , it was found that Cl^- in the electrolyte plays a role in reducing polarization and promoting transport of Zn^{2+} , which plays a synergistic role with the uniform dendrite deposition of Li^+ . Meanwhile, under the condition of 2 M LiCl as the electrolyte additive, the dendrite particles of the zinc anode were the smallest, and the protrusion growth was more compact when the concentration of the additive LiCl was gradually increased. However, the high concentration brings the problems of increased conductivity, pH and mobility. The results may lead to inhomogeneous current distribution during zinc deposition and thus affect the stability of zinc deposition–dissolution.

Similarly, the superior performance of Mg^{2+} as an ionic additive to increase the battery capacity and lifetime has been investigated. Wang et al. [61] concluded that a large number of existing studies on storage mechanisms for ZIBs are based on the adsorption and desorption of individual ions. To explore the bimolecular adsorption and desorption storage mechanisms, the authors reported an electrolyte system using 0.1 M $MgSO_4$ as an additive, demonstrating three major advantages of Mg^{2+} as an EA. First, Mg^{2+} with low reduction potential achieved by Nernst equation adsorbs on the anode surface protrusion, forming an electrostatic shielding effect and promoting the uniform deposition of Zn^{2+} , as shown in Figure 7. The adsorption energy on the Zn surface via DFT exhibits a lower E_{ads} of $MgSO_4$ (-1.953 eV) than that of $ZnSO_4$ (-0.472 eV), demonstrating that Mg^{2+} is preferentially adsorbed on Zn anode (Figure 7b). Meanwhile, the addition of $MgSO_4$ makes the bound water dominated by the local electric field and decreases the free water activity via suppressing the vibration of H_2O molecules, which reduces the occurrence of parasitic reactions. Finally, the battery system with the addition of Mg^{2+} increases the capacity by about 50% extra compared with the initial sample, and the capacity retention rate is 98.7% after 10,000 cycles, which provides a new idea for long-life energy storage devices.

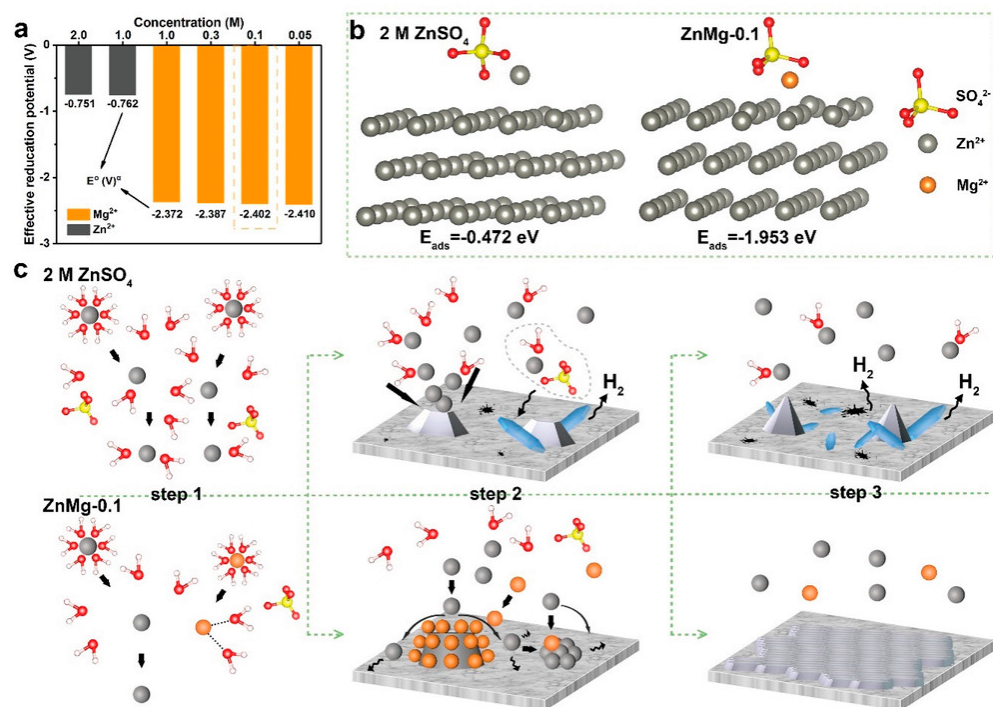


Figure 7. The interaction between the electrolyte and Zn anode. **(a)** Effective reduction potentials of Zn^{2+} and Mg^{2+} at different concentrations. **(b)** Adsorption of electrolyte ions on a Zn surface and corresponding adsorption energy (E_{ads}). **(c)** Schematics of Zn deposition process in the $2\text{ M }ZnSO_4$ (top row) and $ZnMg-0.1$ (bottom row) electrolyte. Reproduced with permissions from Ref. [61]. Copyright © 2021 WILEY-VCH.

Usually, elemental Al is employed as a dopant in cathode materials to boost the stability of the cathode structure [71–73]. Zhou et al. [68] took note of the outstanding properties of Al^{3+} in cathode structure and anode adsorption, and proposed a hybrid multi-electrolyte system with Al^{3+} as an additive. The electrostatic shielding effect was achieved by introducing Al^{3+} to mitigate the production of zinc dendrites, where the insulating basic zinc salts on the cathode significantly decreased. It was further found that the $Zn/K_{0.51}V_2O_5$ cell containing Al^{3+} additive exhibited an impressive cycle time of over 1600 h with a high capacity retention of 91%, which was three times the lifetime of the pure Zn^{2+} electrolyte. By contrast, the capacity of the pure Zn^{2+} electrolyte degraded 65% after 12 cycles at 100 mA g^{-1} . The electrochemical window was increased from 3 V to 4.35 V in

the presence of Al^{3+} , and the excellent cycle stability proved that Al^{3+} is an effective means of electrolyte additive to enhance the long-term stability under low current density.

The anions, including Br^- , I^- , and I_3^- , exhibit suitable redox potentials and good cyclic durability, which could be also developed as an additive in ZIBs [74–76]. Liu et al. [69] introduced I_3^- as an ionic additive into the electrolyte and found that the oxidizing I_3^- could react with Zn^{2+} , where the passivation effect of the Zn anode surface by the oxidizing I_3^- prevented the rapid evolution of detrimental Zn dendrites while concurrently inhibiting corrosion and HER. The fresh Zn in $\text{ZnSO}_4 + \text{KI}$ cell failed after 180 h, while the cell with I_3^- -pretreated Zn electrodes still worked even after 400 h, as displayed in Figure 8a. The reaction between I_3^- and Zn could preferentially remove the sites with high reactivity and high surface area on the Zn anode, which could easily offer a convenient environment for the generation of Zn dendrites. As a result, the uniform deposition of Zn^{2+} was achieved with the help of I_3^- . Meanwhile, the reaction between I_3^- and Zn also competed with the side reaction, where the competing reaction changed the morphology of $\text{Zn}_4(\text{OH})_6\text{SO}_4 \cdot x\text{H}_2\text{O}$ layer and reduced the occurrence of side reaction, as depicted in Figure 8d–e. Unfortunately, it is difficult for I_3^- to form a dense protective film, and the long-term loss of zinc anode is unavoidable; the solution can only be an effective supplement to solve the zinc dendrite problem.

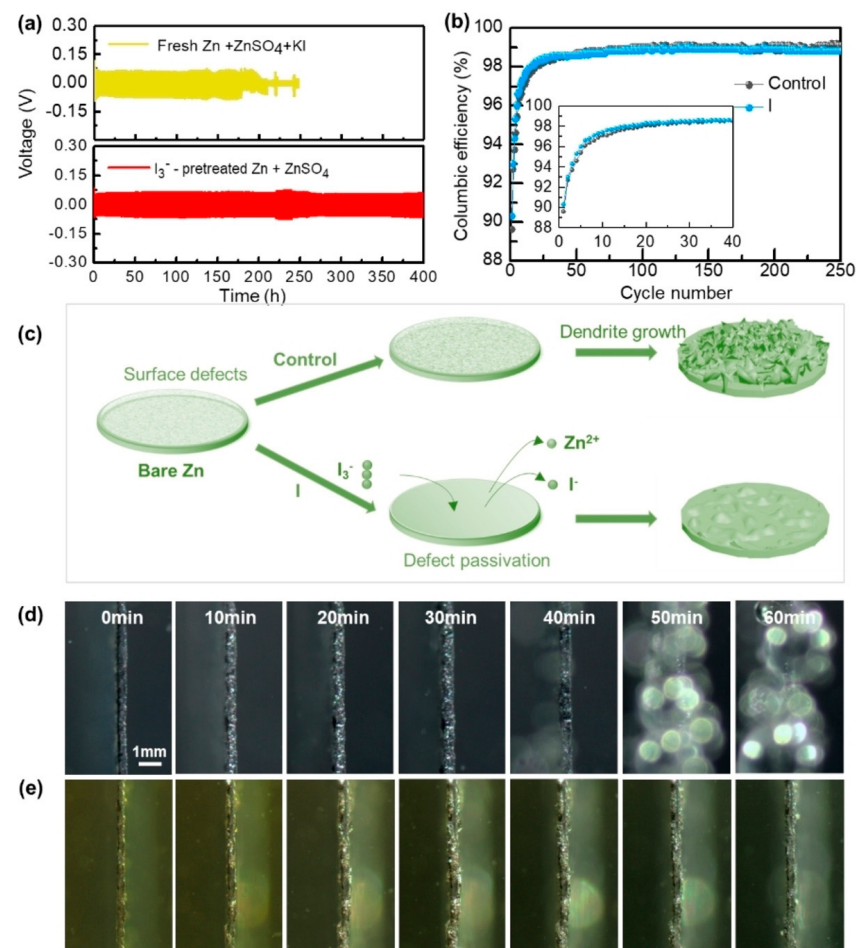


Figure 8. (a) The voltage profiles of Zn/Zn symmetric cells with either fresh Zn in $\text{KI} + \text{ZnSO}_4$ electrolyte or I_3^- -pretreated Zn in ZnSO_4 electrolyte; (b) Coulombic efficiencies of Zn/Cu symmetric cells in either control- or I electrolyte at a current density of 0.25 mA cm^{-2} . (c) Schematic illustration showing the effects of the I_3^- additive on Zn electrodes' striping/plating process. Optical micrographs of Zn^{2+} deposition behavior in: (d) control- and (e) I electrolyte. Reproduced with permissions from Ref. [69]. Copyright © 2022 WILEY-VCH.

From the above examples, it can be seen that ionic additives with simple preparation and superior performance have been extensively developed in various types of energy storage systems, improving the ionic conductivity of the electrolyte and building a dendrite-free ZIB system with the synergistic effect of other ions. However, it should be noted that ionic additives are greatly affected by the concentration of the additive, and the Coulombic efficiency is commonly under low concentration of additives. Additionally, some ions react easily with ions in common electrolytes, and few systems are applicable. The possibility of other ions in inhibiting zinc dendrites should be explored subsequently.

3.3. Organic Additives

In addition to the above-mentioned ionic additives, organic additives are also a common subject of additives and have been broadly studied due to the diversity of organic additive types and functions. Organic additives could deliver abundant diversity, which are divided into five categories, namely small molecules, polymers, ionic, organic acids, and surfactants [77,78]. For example, gelatin [63], thiourea derivatives [79], polyethyleneimine [80], organic dimethyl carbonate [81,82], tetrasodium EDTA [32], alcohols [57], ammonium acetate [83], ethylene diene [84], N-methyl-2-pyrrolidone [65], amino acids [85,86], and other organic solvents [87,88] have played a positive role in solving the Zn dendrite problems. The mechanisms mainly undergo adsorption at the tip to form an electrostatic barrier, the regulation of Zn^{2+} flux to achieve uniform deposition, the improvement of the solvated structure of Zn^{2+} to reduce side reactions, etc. [82,89–93]. The following are examples of the mechanisms of action of organic additives. The function of organic additives is summarized in Table 2.

Table 2. Organic additives and effects in ZIBs.

Solution with Additives	Effects	Operation Parameters and Results	Ref.
2 M $NH_3 \cdot H_2O$ + 4 M NH_4Cl + 20 g L ⁻¹ Zn^{2+} + 5 mM methylthiourea	Inhibit the growth of zinc dendrites Get smooth deposits	-	[79]
0.5 M $ZnSO_4$ + 30 ppm polyethyleneimine	Proceed with a homogenous dissolution Improve the zinc deposition kinetics and morphology	-	[94]
2 M $Zn(OTf)_2$ in molar ratio of H_2O :dimethyl carbonate = 4:1	Form a SEI layer on the Zn electrode	5 mA cm ⁻² @ 2.5 mAh cm ⁻² , 800 h	[81]
2 M $Zn(OTf)_2$ + 7 M diethyl carbonate	Hydrophobic organic cosolvent Reduce the solvating H_2O number Weak water activity Suppress the interfacial side reactions Dominant active sites for H_2 generation Inhibit water electrolysis Promotes desolvation of $Zn(H_2O)_6^{2+}$ Improve the solvation structure	5 mA cm ⁻² @ 2.5 mAh cm ⁻² , 3500 h	[82]
1 M $ZnSO_4$ + 75 mM Na_4EDTA	Inhibit water electrolysis Promotes desolvation of $Zn(H_2O)_6^{2+}$ Improve the solvation structure	5 mA cm ⁻² @ 2 mAh cm ⁻² , 2500 cycles	[32]
1 M $ZnSO_4$ + 0.5 M sorbitol	Restrict all kinds of side reactions Induce the final exposure of the crystal plane (002) with lowest growth rate	1 mA cm ⁻² @ 1 mAh cm ⁻² , 1000 h	[57]
2 M $ZnSO_4$ + 0.2 M CH_3COONH_4	Promote the homogenization of zinc deposition Inhibit the formation of by-products Restrains the increase in local pH	2 mA cm ⁻² , 2400 h	[83]
2 M $ZnSO_4$ + 0.5 M $MnSO_4$ + 6% (w/v) ethylene carbonate	Suppress dendrite formation Inhibit the parasitic reactions on the Zn anode	0.2 mA cm ⁻² @ 0.035 mAh cm ⁻² , 280 h	[84]
0.5 M $ZnCl_2$ + 1 M triethylmethyl-ammonium chloride	Homogenize zinc deposition via adsorbing onto the zinc metal surface Inhibit the formation of by-products by participating in the constitution of contact ion pairs Restrict the 2D diffusion of Zn^{2+} ions	1 mA cm ⁻² @ 0.5 mAh cm ⁻² , 2145 h	[65]
3 M $ZnSO_4$ + 0.1 M threonine	Facilitate the homogeneous deposition of Zn Suppress HER Inhibit the dendritic growth of Zn	1 mA cm ⁻² @ 1 mAh cm ⁻² , 580 h	[85]

Table 2. Cont.

Solution with Additives	Effects	Operation Parameters and Results	Ref.
ZnSO ₄ + 0.1 M cysteine	Exhibit strong interactions with Zn metal	0.5 mA cm ⁻² @ 0.5 mAh cm ⁻² , 2300 h	[86]
1 M Zn(CF ₃ SO ₃) ₂ in H ₂ O:acetonitrile solution with volume ratio of 3:1	Facilitate the reconfiguration of solvation structures	1 mA cm ⁻² @ 1 mAh cm ⁻² , 1300 h	[87]
0.5 M Zn(OTf) ₂ + trimethyl phosphate-DMC (1:1 by volume)	Accumulate on the Zn surface to shield free water	1 mA cm ⁻² , 5000 h	[88]
3 M Zn(CF ₃ SO ₃) ₂ + 0.5 wt% FI	Suppress hydrogen evolution	1 mA cm ⁻² @ 0.5 mAh cm ⁻² , 4000 h	[59]
2 M ZnSO ₄ + 8mg mL ⁻¹ polyaspartic acid	Improve the homogeneity of Zn substrate	0.5 mA cm ⁻² @ 0.5 mAh cm ⁻² , 3200 h	[95]
2 M ZnSO ₄ in 20 vol% dimethyl sulfoxide	Formation of Zn ₃ (PO ₄) ₂	1 mA cm ⁻² @ 1 mA h cm ⁻² , 2100 h	[96]
1 M Zn(CF ₃ SO ₃) ₂ with weight ratio of polyethylene glycol 45%	Anchor on the surface of the Zn electrode to create an interface protective layer	0.25 mA cm ⁻² @ 0.125 mAh cm ⁻² , 1500 h	[97]
1 M ZnSO ₄ with propylene glycol volume fraction 10%	Regulate the Zn ²⁺ solvation shell in the electrolyte	1 mA cm ⁻² @ 1 mAh cm ⁻² , 1025 h	[98]
	Adjust the morphology of the deposited metal zinc		
	Alleviate the side reactions		
	Inducing the fine-grained deposition manner		
	Resist side reactions and dendrite formation		
	Tailor the solvation sheath of Zn ²⁺ and the intensity of hydrogen bonding		
	Favor oriented deposition (002) plane with the low surface energy		
	Regulate the Zn deposition morphology		
	Self-organize into a hydrophobic film		
	Facilitate H ₂ removal from the Zn surface		

The strong interaction between zinc ions and water molecules affects the Zn²⁺ desolvation and nucleation process in conventional electrolytes, which results in the disordered growth of zinc dendrites. The solvated sheath generated by [Zn(H₂O)₆]²⁺ can be further hydrolyzed by Zn²⁺ to produce [Zn(OH)]⁺ and H⁺, which will lead to the formation of zincate by-products and corrosion [39]. Organic additives are rich in functional groups that can improve the desolvation process of Zn²⁺ by interacting with H₂O and Zn²⁺. A safe, low toxicity, and low-cost organic additive to achieve the inhibition of Zn dendrites using fibronectin (FI) that are rich in functional groups (-NH, -OH and -CO) was proposed by Zhu et al. [59]. As displayed in Figure 9, the abundant functional groups not only allowed the FI molecules to adsorb on the anode in a targeted position model, creating an interfacial protective layer, but also interacted with H₂O, thereby modulating the solvated sheath structure of Zn²⁺, achieving uniform and dense deposition of Zn on the anode and reducing the occurrence of side reactions. The composed Zn//Zn full cell retained 98.4% capacity after 1000 cycles at 5 A g⁻¹ with a high Coulombic efficiency of 99%, demonstrating the excellent performance of organic additives in improving the solvated sheath structure of Zn²⁺ and inhibiting Zn dendrites.

The use of organic additives can achieve the modification of the morphology of Zn deposition to overcome the fragile and excessively long structural properties of Zn dendrites and make them small and dense. Zhou et al. [95] developed an organic additive, polyaspartic acid (PASP), to effectively alleviate two major problems of Zn anodes in ZIBs. On the one hand, PASP, as a macromolecular organic compound, could achieve the binding of Zn²⁺ on Zn anode and realize the transformation of Zn²⁺ deposition from a large and brittle dendritic structure to a small and homogeneous spherical structure, as presented in Figure 10. PASP could also form competitive adsorption on H₂O, which inhibited the side reaction between Zn anode and H₂O, reducing the corrosion effect on Zn anode. The addition of PASP enabled the Zn//Zn symmetric cell to realize a long cycle life of 3200 h and 2600 h at 0.5 and 1 mA cm⁻² current densities, respectively, suggesting that PASP as an organic additive is an effective improvement solution.

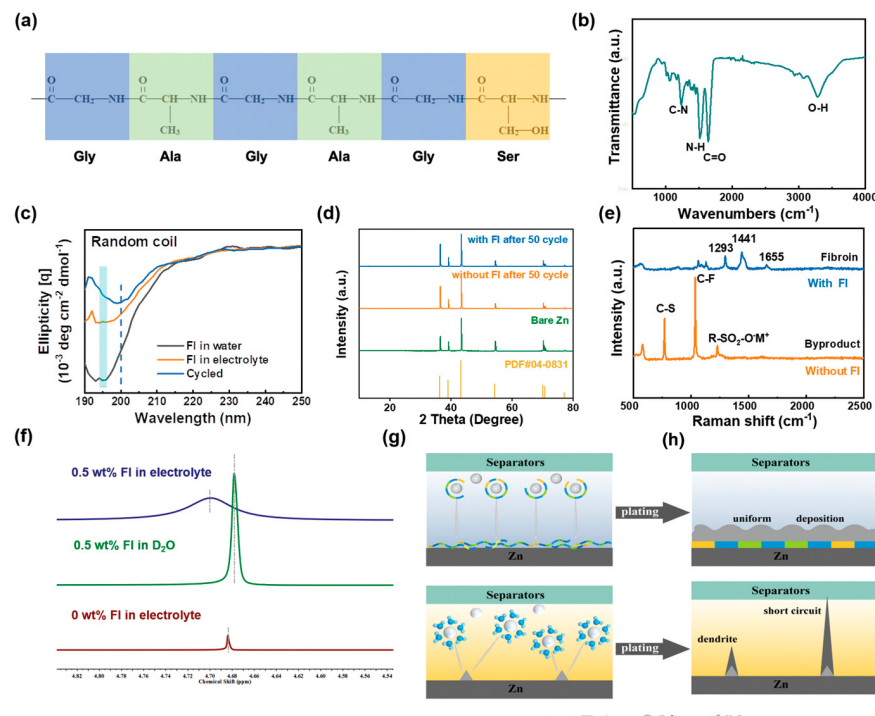


Figure 9. (a) Scheme of fibroin primary structure. (b) The Fourier transform infrared spectroscopy (FT-IR) spectrum of pristine fibroin. (c) The circular dichroic (CD) spectroscopy of FI in water, electrolyte, and cycled. (d) XRD patterns of the Zn electrodes after 50 cycles at 1 mA cm^{-2} (0.5 mAh cm^{-2}) in different electrolytes. (e) Raman spectra of Zn electrodes deposited 100 cycles at 1 mA cm^{-2} (0.5 mAh cm^{-2}) in different electrolytes. (f) Liquid-state ^1H NMR spectra of different solutions with D_2O as solvent. Schematics of Zn^{2+} ion diffusion and reduction progress on the electrode in different electrolytes. (g) With FI additive. (h) Without additive. Reproduced with permissions from Ref. [59]. Copyright © 2022 WILEY-VCH.

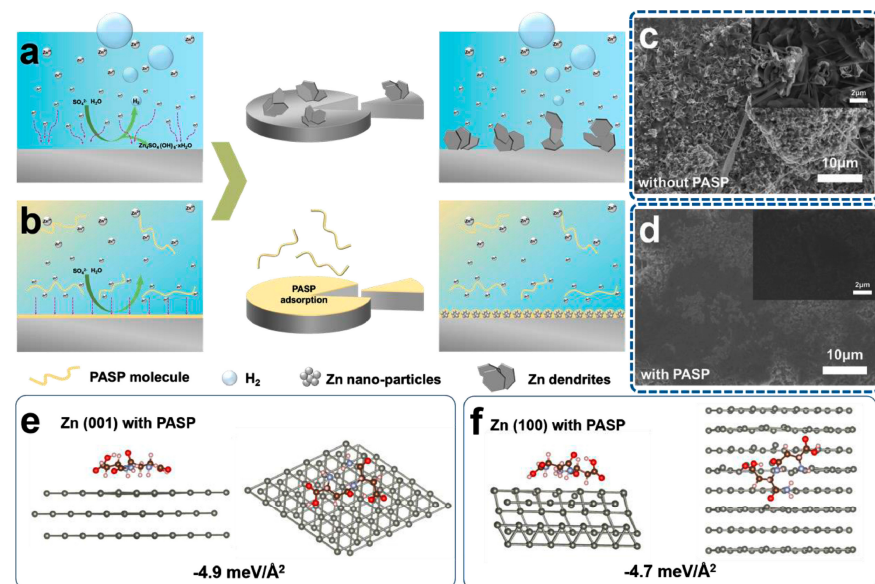


Figure 10. Schematic illustration for the metal Zn deposition process in the electrolyte (a) without or (b) with Pasp additive. The surface of the Zn metal anode deposited at 1 mA cm^{-2} with capacity of 1 mAh cm^{-2} (c) without or (d) with Pasp additive. (e,f) Comparison of the surface energies for the Zn (001) and Zn (100) after Pasp adsorption. Reproduced with permissions from Ref. [95]. Copyright © 2022 Elsevier Ltd.

Organic additives could suppress the generation of Zn dendrites via regulating the Zn^{2+} deposition orientation. Feng et al. [96] conducted a series of studies on dimethyl sulfoxide (DMSO) as an additive and found that DMSO exhibited a higher binding energy with Zn^{2+} than H_2O , and the binding energy disrupted the solvated sheath structure of $[Zn(H_2O)_6]^{2+}$, avoiding the Zn^{2+} deposition process from side reactions with H_2O , as shown in Figure 11. DMSO could provide large adsorption energy for Zn (002) plane for the regulation of Zn^{2+} deposition orientation, and Zn^{2+} was deposited laterally along (002) plane compared with the longitudinal deposition of Zn^{2+} in (101) plane without the addition of DMSO. The surface adsorption energy of DMSO for (002) plane was higher than that of H_2O , which made it easier to expose (002) plane during Zn^{2+} deposition and reduce the generation of dendrites and parasitic reactions. In addition, the experimental Zn // Zn pair cells could last for 1200 h at $-20^{\circ}C$ without dendrites and by-products production due to the hydrogen bonding between DMSO and H_2O , which led to a lower zero point of the electrolyte.

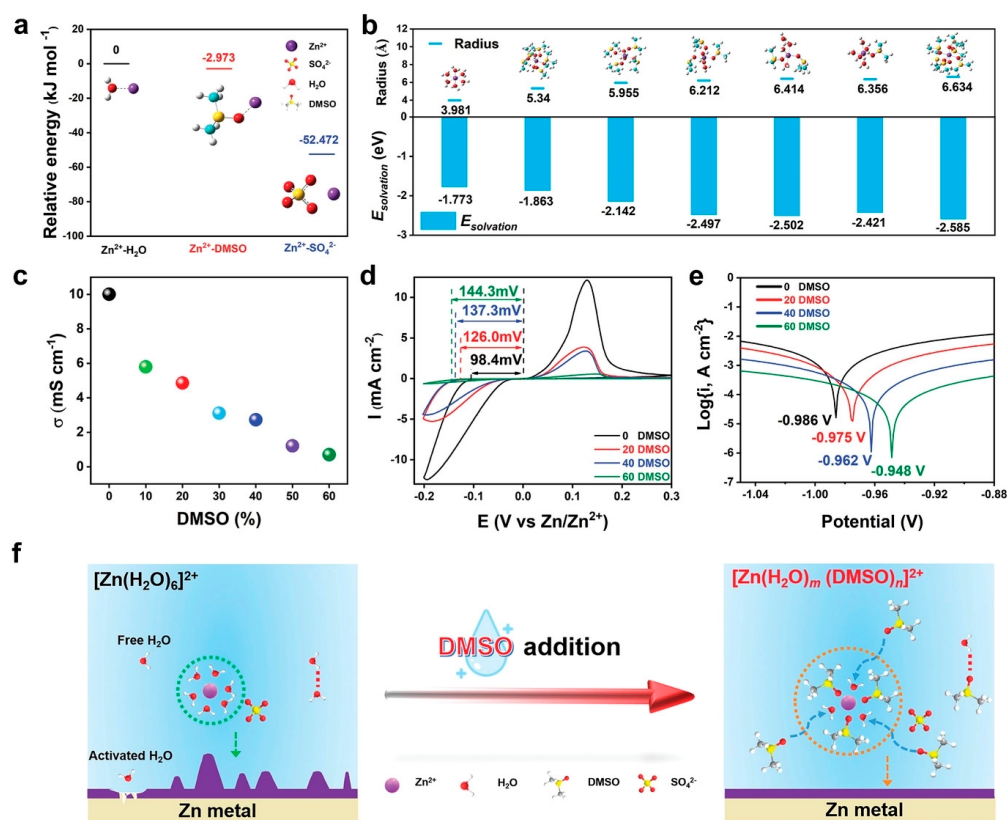


Figure 11. (a) DFT calculations for the relative binding energy of Zn^{2+} to solvent and SO_4^{2-} . (b) The radii and solvation energies of Zn^{2+} with different solvation structures. (c) Ionic conductivities of aqueous electrolyte and DMSO hybrid electrolytes at $20^{\circ}C$. (d) Cyclic voltammetry curves of the Zn electrode in different electrolytes. (e) Tafel curves of the Zn electrode in different electrolytes. (f) Conceptual diagrams of the Zn^{2+} solvation structure and HBs evolution from aqueous electrolyte to DMSO hybrid electrolytes. Reproduced with permissions from Ref. [96]. Copyright © 2021 WILEY-VCH.

Alcohols are regarded as important additives in ZIBs, benefitting from the rich hydroxyl groups [99–102]. Cao et al. [97] proposed a new electrolyte system with 1 M $\text{Zn}(\text{CF}_3\text{SO}_3)_2$ as zinc salt and polyethylene glycol (PEG) as additive to investigate the improvement of Zn^{2+} deposition orientation. In PEG45 electrolyte, the solvent sheath of Zn^{2+} and the strength of hydrogen bonding could be reasonably controlled by PEG molecules, reducing the binding of Zn^{2+} to H_2O . On the other hand, DFT calculations in Figure 12 revealed that the adsorption energy of a single Zn atom on the (002) surface was smaller

than that on the (101) surface, and the addition of PEG facilitated the targeted deposition of Zn^{2+} in the (002) plane with low surface energy during anodic deposition, reducing the generation of dendrites and side reactions. The cell exhibited a long cycle life of up to six times compared to the electrolyte without PEG addition, which opens up new ideas for the subsequent development of stable Zn anodes.

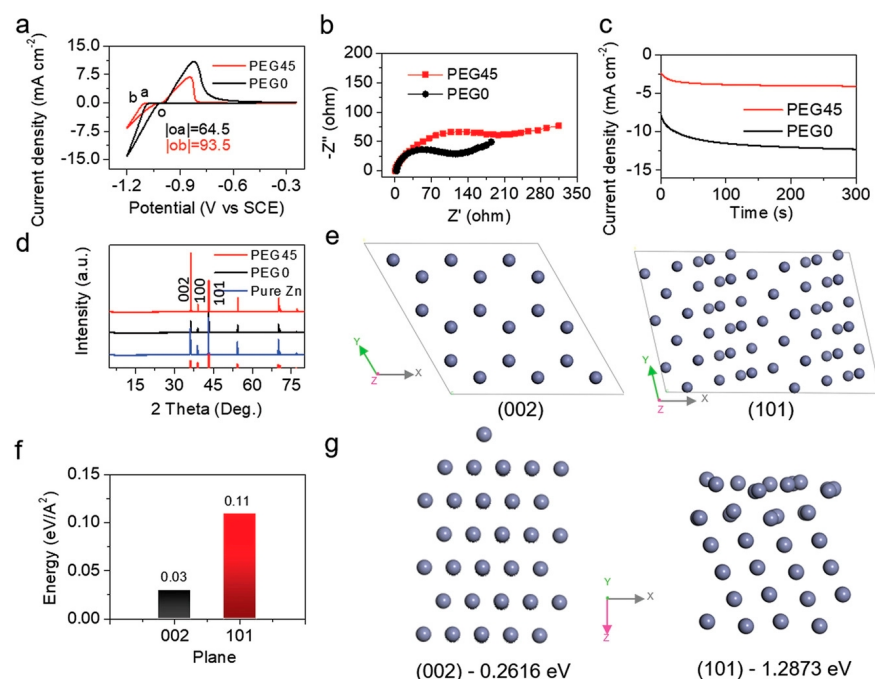


Figure 12. (a) CV curves of Zn nucleation on bare Ti foil in the various electrolytes. (b) EIS of Zn//Zn cells with various electrolytes. (c) Chronoamperograms of Zn foil in PEG0 and PEG45 at -150 mV overpotential. (d) XRD patterns of Zn//Zn cells in PEG0 and PEG45 after 100 cycles at 0.25 mA cm⁻² and 0.125 mAh cm⁻². (e) Distribution of atoms at the plane (002) and (101). (f) Surface energy for the plane (002) and (101). (g) Adsorption energy calculations of free zinc atom at the plane (002) and (101). Reproduced with permissions from Ref. [97]. Copyright © 2022 WILEY-VCH.

Although organic additives are a practical and effective EA, excessive amounts are not encouraged. High concentrations of organic additives, although achieving superior performance, sacrifice the advantages of aqueous ZIBs and are likely to increase the polarization loss at the electrode. Hence, low concentrations of organic additives with high efficiency should be chosen as much as possible. Shang et al. [98], taking into account of the double-side nature of organic additives, introduced a propylene glycol (PG), commonly used in food and medicine, as a non-toxic organic additive. At low concentrations, like other Zn dendrite deposition regulators, PG adsorbed onto protrusions and reactive crystal degree sites and regulated the Zn deposition rate, achieving uniform Zn growth. At the same time, PG changed the solvanted sheath structure of Zn^{2+} , replaced part of H_2O , and the hydrogen bonding formed with the remaining H_2O reduced the activity of H_2O . As described in Figure 13, the low concentration of PG also formed a hydrophobic film spontaneously, which discharged the generated H_2 from the anode surface, thus effectively inhibiting the hydrogen evolution side reaction. Under the high loading of cathode materials, the electrolyte systems with PG addition also presented good stability, and PG has great potential as a low concentration organic additive.

In conclusion, organic additives, as one of the commonly used EAs, are rich in functional groups that can realize the formation of ligands with Zn^{2+} or H_2O , and play a positive role in synergistically regulating the Zn deposition orientation and improving the solvation structure of Zn^{2+} [103]. Most of the organic additives exist in the form of organic molecules, and the strong interaction between Zn^{2+} and the additives will increase the

Zn nucleation overpotential, while the formation of solvated sheath structures with larger radius requires more energy to destroy, which brings greater obstacles to the process of Zn^{2+} desolvation and ion diffusion. As for some organic additives, the increase in the concentration will bring toxic and flammable safety hazards, increase the viscosity of the electrolyte, reduce the electrode conductivity, and lead to an increase in the resistance of the electrolyte system. The employment of other organic additives with low toxicity and low cost can be explored subsequently to investigate other effects of organic additives on Zn-ion batteries.

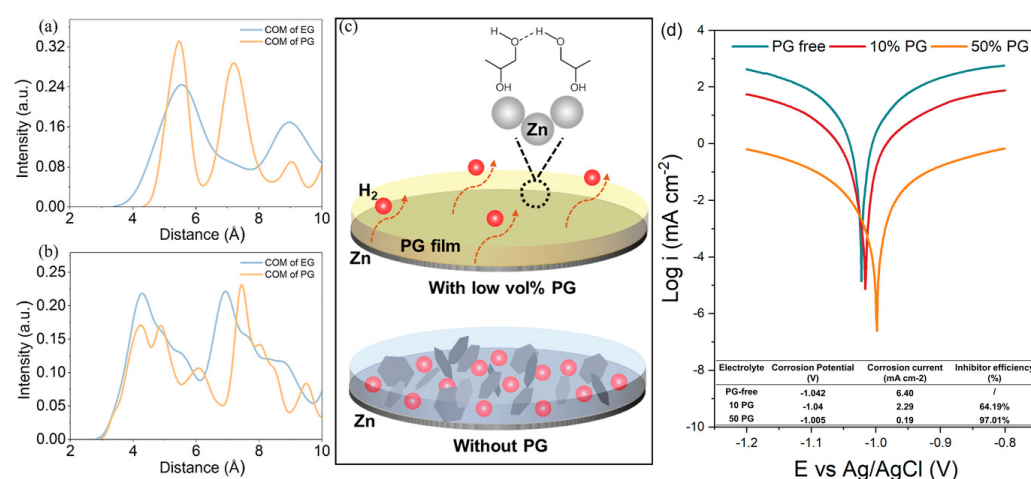


Figure 13. Ab initio molecular dynamics simulation of the concentration-dependent effectivity of PG. Distributions for the PG/EG center of mass (denoted as COM) distance at (a) low and (b) high concentrations. The appearance of well-defined sharper peaks for PG at the low concentration indicates self-organization mediated film formation (as depicted in (c)) that owing to hydrophobic nature ($-\text{CH}_3$ tail and hydrocarbon backbone) can remove the hydrogen bubbles from the zinc surface that in the PG free electrolyte induces porous and flaky zinc deposit formation. (d) Tafel plots obtained for the PG-free, 10% PG, and 50% PG electrolytes with the corresponding corrosion potential, corrosion current density, and inhibitor efficiency listed in inset table. Reproduced with permissions from Ref. [98]. Copyright © 2022 WILEY-VCH.

3.4. Inorganic Additives

Compared with ionic and organic additives, in general, there are few studies on inorganic additives, which are still under difficult exploration since the own solubility and variety are limited. Here, the soluble concentration is normally determined at the mmol L^{-1} level. Despite its solubility being extraordinarily low relative to ionic and organic additives, its great influence on anode properties has been demonstrated [104]. Inorganic additives are mainly divided into three types: oxide, inorganic acid, and other materials. For example, phosphoric acid, tartaric acid, and succinic acid used as inorganic additives have been experimented in zinc-air batteries [105], and it was found that in the presence of citric acid, neither needles nor dendrites were formed and the zinc deposition was very compact. Additionally, inorganic materials, including 2D materials and nanoparticles, were also employed as typical electrolyte additives in ZIBs [106]. Table 3 summarizes the typical inorganic additives and their role in zinc dendrites.

Unlike the scheme of directly applying SEI layers to the anode, Huang et al. [107] artificially constructed an *in situ* inorganic SEI protective layer by introducing SeO_2 as an inorganic additive into 2 M ZnSO_4 . In fact, SeO_2 underwent a hydrolysis reaction in the electrolyte and eventually formed SeO_3^{2-} ions before the plating. The SeO_3^{2-} ions derived from SeO_2 could combine and react with Zn^{2+} to *in situ* generate an inorganic ZnSe protective layer. Meanwhile, the strong affinity between ZnSe and Zn allowed Zn to be deposited uniformly on the protective layer, while the self-healing ability of the ZnSe layer reduced the cracks caused by the expansion of the deposited volume, ensuring the

durability of the ZnSe layer, as shown in Figure 14. The formed SeO_3^{2-} ion could also react with H^+ , which enhances the corrosion resistance of the electrode. The lifetime of the Zn//Zn symmetric cell was measured to be as long as 2100 h at 2 mA cm^{-2} , and the Coulomb efficiency of the Zn/Cu half-cell also reached 99.6%. The experimental data confirmed that the ZnSe protective layer constructed via SeO_2 as an additive is superior to the coating prepared by vapor deposition, demonstrating the good performance of SeO_2 as an inorganic additive.

Table 3. Inorganic additives and effects in ZIBs.

Solution with Additives	Effects	Operation Parameters and Results	Ref.
2 M ZnSO_4 + 2 mM SeO_2	Form ZnSe protective layer Promote the nucleation and growth Self-healing	2 mA cm^{-2} @ 2 mAh cm^{-2} , 2100 h	[107]
3 M ZnSO_4 + 0.1 M MnSO_4 + 0.5 mg ml^{-1} TS-Ns	attract plenty of Zn ions from electrolyte Increase local Zn^{2+} ion Reduce Zn nucleation overpotential	1 mA cm^{-2} @ 1 mAh cm^{-2} , 480 h	[108]
2 M ZnSO_4 + 0.05 M $\text{Ti}_3\text{C}_2\text{T}_x$ Mxene	Uniform initial Zn deposition via providing abundant zincophilic-O groups Form robust solid-electrolyte interface	1 mA cm^{-2} @ 1 mAh cm^{-2} , 500 cycles	[109]
2 M ZnSO_4 + 0.4 g L^{-1} graphene quantum dots	Strong coordination interactions between GQDs and Zn^{2+} ions Promote homogeneous Zn^{2+} ions distribution Accelerate the Zn^{2+} deposition kinetics	0.8 mA cm^{-2} @ 0.2 mAh cm^{-2} , 2200 h	[110]

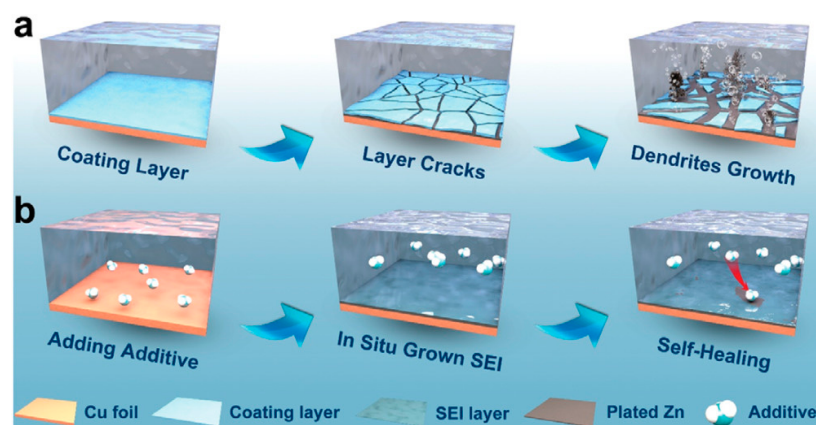


Figure 14. Schematic diagram showing Zn deposition using (a) coating layer and (b) SEI-forming additive strategy. Reproduced with permissions from Ref. [107]. Copyright © 2022 WILEY-VCH.

Another major class of inorganic additives that are more frequently used are 2D nanosheet materials, which possess the merits of adjustable volume, larger lateral dimensions and easily exposed active sites, non-toxicity and environmental friendliness over other additives. Zhang et al. [108] investigated 2D ultrathin anionic tin sulfide nanosheets (TS-Ns) and elucidated the mechanism that drives the homogeneous deposition of Zn^{2+} . Initially, the TS-Ns with negative charge attracted a large number of positive Zn^{2+} on the surface via electrostatic interaction and increased the local concentration of Zn^{2+} . Then, Zn^{2+} was co-deposited on the anode surface together with TS-Ns, which was confirmed by the XPS spectrum and SEM mapping of the sample after stripping. As a result, an interfacial protective layer was formed near the Zn anode to guide the distributed deposition of Zn and reduce the generation of Zn dendrites, as depicted in Figure 15. The cycle life of the Zn/Zn symmetric cell with TS-Ns as an additive exceeded 1850 cycles without short circuit. The experiment exhibits a good inhibition of Zn dendrites under the co-deposition of TS-Ns and Zn, which opens up new ideas for the selection of inorganic additives.

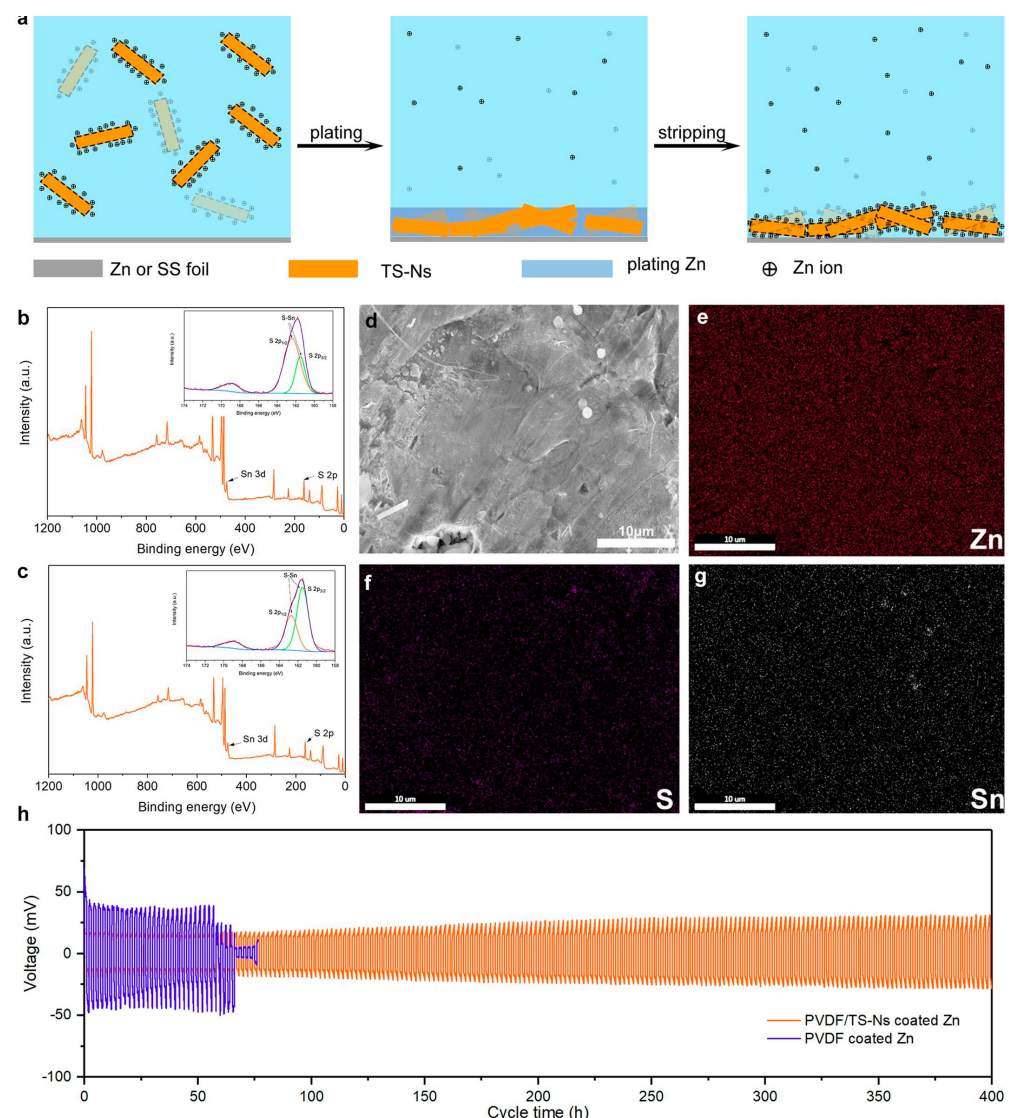


Figure 15. (a) Schematic illustration of the working mechanism of TS-Ns participated in the Zn plating/stripping. (b) XPS pattern of Zn foil after plating for 0.5 mAh cm^{-2} at 0.1 mA cm^{-2} . An inset is high resolution XPS spectra of S 2p. (c) XPS pattern of Zn foil after plating for 0.5 mAh cm^{-2} and then stripping for 0.5 mAh cm^{-2} . An inset is high resolution XPS spectra of S 2p. (d–g) SEM image and EDX mapping of Zn foil after plating for 0.5 mAh cm^{-2} and then stripping for 0.5 mAh cm^{-2} . (h) The voltage profiles of the symmetric cells composed of the PVDF/TS-Ns-coated Zn and the PVDF-coated Zn at 1 mAh cm^{-2} and 1 mA cm^{-2} . Reproduced with permissions from Ref. [108]. Copyright © 2022 Elsevier Ltd.

MXene emerges as a new type of compelling two-dimensional materials, which exhibits the distinctive properties of high surface area, abundant surface functional groups, metallic conductivity, strong hydrophilicity and good chemical stability [111]. Inspired by previous work involving ideal hosts for dendrite-free Li/Na/K anode [112,113], Sun et al. [109] proposed $\text{Ti}_3\text{C}_2\text{T}_x$ MXene as an EA to ameliorate problems, such as anode Zn dendrites and parasitic reactions. The MXene could be adsorbed on the Zn anode to induce the uniform Zn deposition via the abundant zincophilic-O groups and subsequently participated in the formation of robust solid-electrolyte interface layer. The binding energies between -OH, -F and -O groups and metal Zn substrates were -7.64 , -18.35 and -26.33 eV, respectively, revealing the powerful adhesive tendency between MXene and Zn foil, as described in Figure 16c,d. The generated MXene-Zn²⁺ functional layer

could also homogenize the dispersion of surface Zn^{2+} and provide well-dispersed “seed points” to induce uniform nucleation and homogenous ionic flux in the deposition process, suppressing the growth of Zn dendrites. At 2 mA cm^{-2} , the Zn/Zn cell exhibits a stable cycling performance up to 1100 cycles and a high Coulomb efficiency (99.7%).

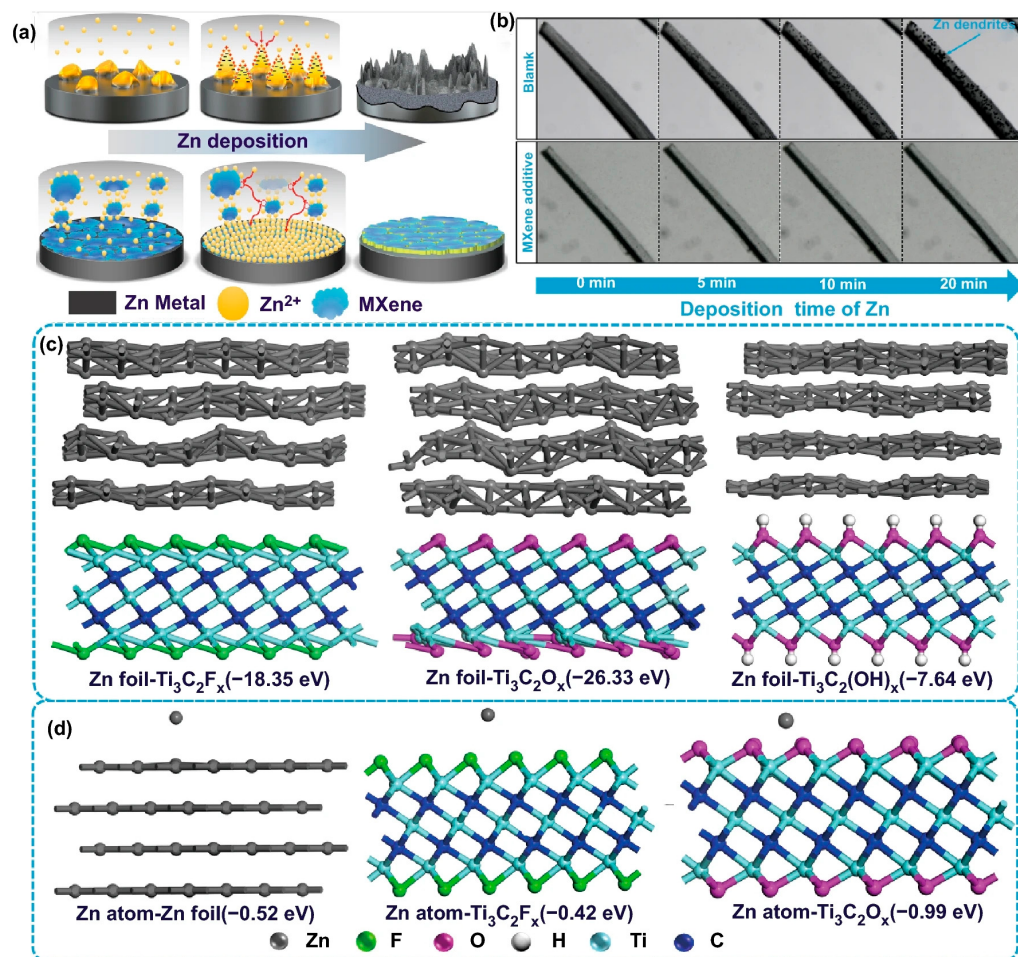


Figure 16. (a) Schematic illustration of the effect of MXene additive on the Zn deposition process. (b) In situ optical microscopy observation of Zn deposition at 4 mA cm^{-2} in blank ZnSO_4 electrolyte and MXene-added electrolyte. Density functional theory calculation models of (c) $\text{Ti}_3\text{C}_2\text{T}_x$ adsorbed on Zn foil and (d) Zn atoms absorbed on Zn foil, $\text{Ti}_3\text{C}_2\text{T}_x$ and the corresponding binding energies. Reproduced with permissions from Ref. [109]. Copyright © 2021 Springer-Verlag London Ltd.

In addition, graphene-based materials including graphene quantum dots (GQDs) and graphene oxide with abundant functional groups and low toxicity at the quantum level have also been favored by many researchers [114]. Zhang et al. [110] prepared GQDs using lower cost graphite powder, which was introduced into the ZnSO_4 electrolyte. As a result, electrochemically stable Zn anode was successfully constructed via manipulating the nucleation process through the introduction of hydrophilic GQDs. According to DFT analysis in Figure 17a, GQDs exhibited a stronger adsorption of Zn^{2+} by the rich-oxygen groups, which makes GQDs a medium to guide homogeneous Zn deposition during the repeated cycling process. The possible mechanism of GQDs in the electroplating process of zinc anode is elucidated in Figure 17b. GQDs could preferentially absorb the tip with higher potential at the anode surface and dissolve in the electrolyte. The lower nucleation potential helps to increase the nucleation sites, and the stronger binding energy oxygen-containing groups could adsorb Zn^{2+} to induce uniform zinc deposition. This makes Zn^{2+} tend to deposit on the anode surface and effectively inhibits the growth of zinc dendrites.

At 0.8 mA cm^{-2} , the Zn//Zn symmetric cell exhibited a long cycle life of 2200 h with a reduced polarization voltage of 50 mV when GQDs (0.4 g L^{-1}) were introduced into the solution. In this research work, the graphene quantum dots demonstrated excellent performance that deserves further exploration.

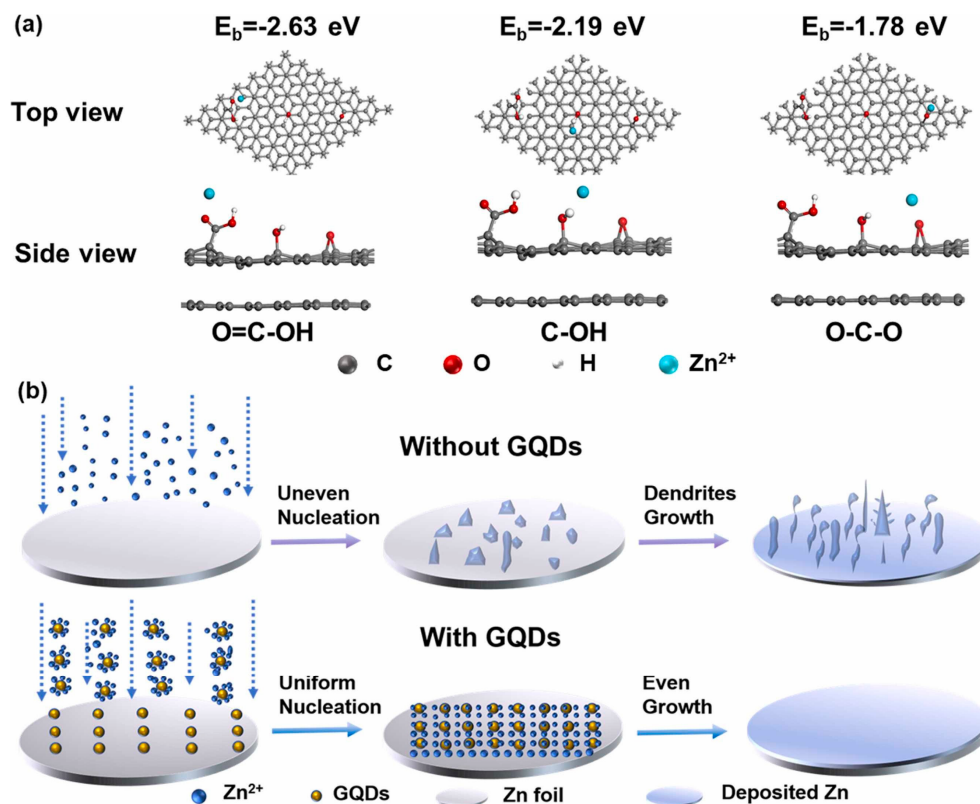


Figure 17. (a) Calculation models of Zn ion absorbed on different oxygen-function groups and corresponding binding energy. (b) Schematic depiction of the effect toward suppressing dendrites growth. Reproduced with permissions from Ref. [110]. Copyright © 2022 Elsevier Ltd.

Currently, the research on inorganic additives to inhibit zinc dendrites is relatively limited due to the low solubility of inorganic substances. On the other hand, the amount of required additives is low, and the high cost will also result in some limitations. Hence, expanding the role of more types of inorganic additives in electrolytes should receive more extensive attention and more in-depth research.

4. Conclusions and Future Perspectives

The simple, safe, and efficient electrolyte additive strategy exhibits a critically important impact on mitigating zinc dendrite growth, reducing side reactions, and improving the performance and lifetime of ZIBs. Compared to other methods, the EA approach is more practical and less costly with improved cycle life and Coulomb efficiency, making the approach easier to apply to large-scale production [52]. However, EA technology currently still encounters some challenges: (1) The role of EAs on electrolytes and cathodes is still unclear; (2) a high amount of additives in electrolyte would bring high cost; and (3) the addition of some additives leads to toxic or flammable electrolyte systems, which is not conducive to environmental protection. Although these problems exist only in some EAs, solving these problems could provide a better understanding of the mechanism of action of electrolyte additives, which is beneficial for improving the selection scheme of EAs and realizing their application in practical scenarios. Based on the systematic discussion of zinc dendrite growth and side reaction mechanisms, we focus on the analysis of the

representative progress of EAs and put forward some constructive suggestions for EA technology to provide directions and ideas for the future development of related research.

Overall, the EA solution achieved good results in solving the zinc dendritic problems, and more mature and effective solutions should be explored to promote the application of experimental research results to practical production. For this reason, the following ideas for follow-up research in electrolyte additives are proposed.

- (1) More in-depth research on inorganic types of electrolyte additives. As mentioned above, the development of diverse low cost and non-toxic inorganic additives may lead to breakthroughs and fundamental improvements in zinc dendritic problems. In the future, inorganic additives with different characteristics could be designed to give full play to their own advantages and explore highly efficient inorganic additives that can minimize dendrite generation and side reactions and optimize battery performance.
- (2) Building mixed electrolyte system and the action mechanism. Currently, most research is limited to adding single component electrolyte additives or complementary additives of the same type in a system, but the exploration of multi-component electrolyte additives added together has not been well carried out, and establishing a link between ionic additives, organic additives, and inorganic additives to achieve synergistic effects in the electrolyte system may become a breakthrough. The influence of multiple additives can reduce the formation of dendrites more efficiently, and it is worthwhile to further study whether different additives can be linked and the mechanism of action.
- (3) Exploring the effect of electrolyte additives on the cathode. While electrolyte additives play the largest role in inhibiting anodic zinc dendrites and side reactions, and the principle and process of action are studied in detail, the effect of EAs on cathode properties has not been well described in the cathode. Therefore, the role of EAs on the cathode of the battery should be noted in the subsequent research to achieve a high level of overall battery performance.
- (4) Development of multifunctional EAs. With the development of flexible devices and low-temperature resistant batteries, a lot of attention has been focused on the wide temperature operating range and ductile energy storage devices, which put forward higher requirements for the electrolytes, and the use of EAs can change the nature of the electrolyte, thereby moving toward multifunctional and high performance. Some EAs can already meet these requirements, but they can be accompanied by problems, such as decreasing conductivity and insufficient mechanical properties, to meet the electrochemical performance and lifetime requirements. Therefore, the material selection and preparation methods of EAs need to be further explored.

Author Contributions: Conceptualization, C.Z. and Y.H.; investigation, C.Z.; resources, B.C., H.H. and Z.G.; data curation, D.Z.; writing—original draft preparation, C.Z. and Y.H.; writing—review and editing, C.Z., Y.H. and X.W.; supervision, Y.H. and X.W.; project administration, H.H.; funding acquisition, Y.H., H.H. and Z.G. All authors have read and agreed to the published version of the manuscript.

Funding: This research was funded by the National Natural Science Foundation of China (22002054, 52064028), Yunnan Provincial Major Science and Technology Special Plan Projects (202202AF080002), Yunnan Fundamental Research Projects (202101AU070157, 202101AS070013), China Postdoctoral Science Foundation (2018M633418), and Analysis and Testing Foundation of Kunming University of Science and Technology (2021T20200004).

Data Availability Statement: Not applicable.

Conflicts of Interest: The authors declare that they have no known competing financial interests or personal relationships that could have appeared to influence the work reported in this paper.

Abbreviations

electrolyte additives	EAs
zinc-ion batteries	ZIBs
li-ion batteries	LIBs
hydrogen evolution reaction	HER
zinc	Zn
water-in-salt electrolyte	WISE
lithium bis(trifluoromethanesulfonimide)	LiTFSI
zinc trifluoromethanesulfonate	Zn(TfO) ₂
X-ray absorption near edge structure	XANES
fibronectin	FI
polyaspartic acid	PASP
dimethyl sulfoxide	DMSO
polyethylene glycol	PEG
propylene glycol	PG
tin sulfide nanosheets	TS-Ns
graphene quantum dots	GQDs

References

1. Bayatsarmadi, B.; Zheng, Y.; Vasileff, A.; Qiao, S.-Z. Recent Advances in Atomic Metal Doping of Carbon-based Nanomaterials for Energy Conversion. *Small* **2017**, *13*, 1700191. [[CrossRef](#)] [[PubMed](#)]
2. Lee, D.U.; Xu, P.; Cano, Z.P.; Kashkooli, A.G.; Park, M.G.; Chen, Z. Recent progress and perspectives on bi-functional oxygen electrocatalysts for advanced rechargeable metal–air batteries. *J. Mater. Chem. A* **2016**, *4*, 7107–7134. [[CrossRef](#)]
3. Tan, K.M.; Babu, T.S.; Ramachandaramurthy, V.K.; Kasinathan, P.; Solanki, S.G.; Raveendran, S.K. Empowering smart grid: A comprehensive review of energy storage technology and application with renewable energy integration. *J. Energy Storage* **2021**, *39*, 102591. [[CrossRef](#)]
4. Perumal, P.; Andersen, S.M.; Nikoloski, A.; Basu, S.; Mohapatra, M. Leading strategies and research advances for the restoration of graphite from expired Li⁺ energy storage devices. *J. Environ. Chem. Eng.* **2021**, *9*, 106455. [[CrossRef](#)]
5. Tian, Y.; Zeng, G.; Rutt, A.; Shi, T.; Kim, H.; Wang, J.; Koettgen, J.; Sun, Y.; Ouyang, B.; Chen, T.; et al. Promises and Challenges of Next-Generation “Beyond Li-ion” Batteries for Electric Vehicles and Grid Decarbonization. *Chem. Rev.* **2021**, *121*, 1623–1669. [[CrossRef](#)]
6. Zhao, F.; Li, Y.; Feng, W. Recent Advances in Applying Vulcanization/Inverse Vulcanization Methods to Achieve High-Performance Sulfur-Containing Polymer Cathode Materials for Li-S Batteries. *Small Methods* **2018**, *2*, 1800156. [[CrossRef](#)]
7. Zhang, S.S. Problem, Status, and Possible Solutions for Lithium Metal Anode of Rechargeable Batteries. *ACS Appl. Energy Mater.* **2018**, *1*, 910–920. [[CrossRef](#)]
8. Gandoman, F.H.; Jaguemont, J.; Goutam, S.; Gopalakrishnan, R.; Firouz, Y.; Kalogiannis, T.; Omar, N.; Van Mierlo, J. Concept of reliability and safety assessment of lithium-ion batteries in electric vehicles: Basics, progress, and challenges. *Appl. Energy* **2019**, *251*, 113343. [[CrossRef](#)]
9. Zhao, F.; Wang, Y.; Zhang, X.; Liang, X.; Zhang, F.; Wang, L.; Li, Y.; Feng, Y.; Feng, W. Few-layer methyl-terminated germanene-graphene nanocomposite with high capacity for stable lithium storage. *Carbon* **2020**, *161*, 287–298. [[CrossRef](#)]
10. Zhang, X.; Hu, J.-P.; Fu, N.; Zhou, W.-B.; Liu, B.; Deng, Q.; Wu, X.-W. Comprehensive review on zinc-ion battery anode: Challenges and strategies. *InfoMat* **2022**, *4*, e12306. [[CrossRef](#)]
11. Zhang, M.; Liang, R.; Or, T.; Deng, Y.-P.; Yu, A.; Chen, Z. Recent Progress on High-Performance Cathode Materials for Zinc-Ion Batteries. *Small Struct.* **2021**, *2*, 2000064. [[CrossRef](#)]
12. Lu, W.; Zhang, C.; Zhang, H.; Li, X. Anode for Zinc-Based Batteries: Challenges, Strategies, and Prospects. *ACS Energy Lett.* **2021**, *6*, 2765–2785. [[CrossRef](#)]
13. Li, Y.; Wang, Z.; Cai, Y.; Pam, M.E.; Yang, Y.; Zhang, D.; Wang, Y.; Huang, S. Designing Advanced Aqueous Zinc-Ion Batteries: Principles, Strategies, and Perspectives. *Energy Environ. Mater.* **2021**, *5*, 823–851. [[CrossRef](#)]
14. Wang, Y.; Wang, Z.; Yang, F.; Liu, S.; Zhang, S.; Mao, J.; Guo, Z. Electrolyte Engineering Enables High Performance Zinc-Ion Batteries. *Small* **2022**, *2107033*. [[CrossRef](#)]
15. Liu, Y.; Liu, Y.; Wu, X. Toward Long-Life Aqueous Zinc Ion Batteries by Constructing Stable Zinc Anodes. *Chem. Rec.* **2022**, *e202200088*. [[CrossRef](#)]
16. Jiao, S.; Fu, J.; Wu, M.; Hua, T.; Hu, H. Ion Sieve: Tailoring Zn²⁺ Desolvation Kinetics and Flux toward Dendrite-Free Metallic Zinc Anodes. *ACS Nano* **2022**, *16*, 1013–1024. [[CrossRef](#)]
17. Jiao, Q.; Zhou, T.; Zhang, N.; Liu, S.; Huang, Q.; Bi, W.; Chu, W.; Wu, X.; Zhu, Y.; Feng, Y.; et al. High-surface-area titanium nitride nanosheets as zinc anode coating for dendrite-free rechargeable aqueous batteries. *Sci. China Mater.* **2022**, *65*, 1771–1778. [[CrossRef](#)]

18. Han, X.; Leng, H.; Qi, Y.; Yang, P.; Qiu, J.; Zheng, B.; Wu, J.; Li, S.; Huo, F. Hydrophilic silica spheres layer as ions shunt for enhanced Zn metal anode. *Chem. Eng. J.* **2022**, *431*, 133931. [[CrossRef](#)]
19. Dai, L.; Wang, T.; Jin, B.; Liu, N.; Niu, Y.; Meng, W.; Gao, Z.; Wu, X.; Wang, L.; He, Z. γ -Al₂O₃ coating layer confining zinc dendrite growth for high stability aqueous rechargeable zinc-ion batteries. *Surf. Coat. Technol.* **2021**, *427*, 127813. [[CrossRef](#)]
20. Wang, Y.; Guo, T.; Yin, J.; Tian, Z.; Ma, Y.; Liu, Z.; Zhu, Y.; Alshareef, H.N. Controlled Deposition of Zinc-Metal Anodes via Selectively Polarized Ferroelectric Polymers. *Adv. Mater.* **2022**, *34*, 2106937. [[CrossRef](#)]
21. Yuan, C.; Yin, L.; Du, P.; Yu, Y.; Zhang, K.; Ren, X.; Zhan, X.; Gao, S. Microgroove-patterned Zn metal anode enables ultra-stable and low-overpotential Zn deposition for long-cycling aqueous batteries. *Chem. Eng. J.* **2022**, *442*, 136231. [[CrossRef](#)]
22. Yun, K.; Jang, H.; An, G.-H. Stable anode enabled by an embossed and punched structure for a high-rate performance Zn-ion hybrid capacitor. *Int. J. Energy Res.* **2022**, *46*, 7175–7185. [[CrossRef](#)]
23. Zhao, K.; Liu, F.; Fan, G.; Liu, J.; Yu, M.; Yan, Z.; Zhang, N.; Cheng, F. Stabilizing Zinc Electrodes with a Vanillin Additive in Mild Aqueous Electrolytes. *ACS Appl. Mater. Interfaces* **2021**, *13*, 47650–47658. [[CrossRef](#)]
24. Hoang, T.K.A.; Acton, M.; Chen, H.T.H.; Huang, Y.; Doan, T.N.L.; Chen, P. Sustainable gel electrolyte containing Pb²⁺ as corrosion inhibitor and dendrite suppressor for the zinc anode in the rechargeable hybrid aqueous battery. *Mater. Today Energy* **2017**, *4*, 34–40. [[CrossRef](#)]
25. Guo, S.; Qin, L.; Zhang, T.; Zhou, M.; Zhou, J.; Fang, G.; Liang, S. Fundamentals and perspectives of electrolyte additives for aqueous zinc-ion batteries. *Energy Storage Mater.* **2021**, *34*, 545–562. [[CrossRef](#)]
26. Zhou, J.; Zhang, L.; Peng, M.; Zhou, X.; Cao, Y.; Liu, J.; Shen, X.; Yan, C.; Qian, T. Diminishing Interfacial Turbulence by Colloid-Polymer Electrolyte to Stabilize Zinc Ion Flux for Deep-Cycling Zn Metal Batteries. *Adv. Mater.* **2022**, *34*, 2200131. [[CrossRef](#)] [[PubMed](#)]
27. Zhang, S.S. A review on electrolyte additives for lithium-ion batteries. *J. Power Sources* **2006**, *162*, 1379–1394. [[CrossRef](#)]
28. Li, C.; Wu, Q.; Ma, J.; Pan, H.; Liu, Y.; Lu, Y. Regulating zinc metal anodes via novel electrolytes in rechargeable zinc-based batteries. *J. Mater. Chem. A* **2022**, *10*, 14692–14708. [[CrossRef](#)]
29. Cao, L.; Skyllas-Kazacos, M.; Menictas, C.; Noack, J. A review of electrolyte additives and impurities in vanadium redox flow batteries. *J. Energy Chem.* **2018**, *27*, 1269–1291. [[CrossRef](#)]
30. Geng, Y.; Pan, L.; Peng, Z.; Sun, Z.; Lin, H.; Mao, C.; Wang, L.; Dai, L.; Liu, H.; Pan, K.; et al. Electrolyte additive engineering for aqueous Zn ion batteries. *Energy Storage Mater.* **2022**, *51*, 733–755. [[CrossRef](#)]
31. Han, M.; Zheng, D.; Song, P.; Ding, Y. Theoretical study on fluoroethylene carbonate as an additive for the electrolyte of lithium ion batteries. *Chem. Phys. Lett.* **2021**, *771*, 138538. [[CrossRef](#)]
32. Zhang, S.-J.; Hao, J.; Luo, D.; Zhang, P.-F.; Zhang, B.; Davey, K.; Lin, Z.; Qiao, S.-Z. Dual-Function Electrolyte Additive for Highly Reversible Zn Anode. *Adv. Energy Mater.* **2021**, *11*, 2102010. [[CrossRef](#)]
33. Kim, J.; Adiraju, V.A.K.; Chae, O.B.; Lucht, B.L. Lithium Bis(trimethylsilyl) Phosphate as an Electrolyte Additive to Improve the Low-Temperature Performance for LiNi_{0.8}Co_{0.1}Mn_{0.1}O₂/Graphite Cells. *J. Electrochem. Soc.* **2021**, *168*, 080538. [[CrossRef](#)]
34. Li, T.C.; Fang, D.; Zhang, J.; Pam, M.E.; Leong, Z.Y.; Yu, J.; Li, X.L.; Yan, D.; Yang, H.Y. Recent progress in aqueous zinc-ion batteries: A deep insight into zinc metal anodes. *J. Mater. Chem. A* **2021**, *9*, 6013–6028. [[CrossRef](#)]
35. He, P.; Chen, Q.; Yan, M.; Xu, X.; Zhou, L.; Mai, L.; Nan, C.-W. Building better zinc-ion batteries: A materials perspective. *Energy Chem.* **2019**, *1*, 100022. [[CrossRef](#)]
36. Sze, Y.-K.; Irish, D.E. Vibrational spectral studies of ion-ion and ion-solvent interactions. I. Zinc nitrate in water. *J. Solut. Chem.* **1978**, *7*, 395–415. [[CrossRef](#)]
37. Beverskog, B.; Puigdomenech, I. Revised pourbaix diagrams for zinc at 25–300 °C. *Corros. Sci.* **1997**, *39*, 107–114. [[CrossRef](#)]
38. Cao, Z.; Zhuang, P.; Zhang, X.; Ye, M.; Shen, J.; Ajayan, P.M. Strategies for Dendrite-Free Anode in Aqueous Rechargeable Zinc Ion Batteries. *Adv. Energy Mater.* **2020**, *10*, 2001599. [[CrossRef](#)]
39. Han, C.; Li, W.; Liu, H.K.; Dou, S.; Wang, J. Principles and strategies for constructing a highly reversible zinc metal anode in aqueous batteries. *Nano Energy* **2020**, *74*, 104880. [[CrossRef](#)]
40. McLarnon, F.R.; Cairns, E.J. The Secondary Alkaline Zinc Electrode. *J. Electrochem. Soc.* **1991**, *138*, 645–656. [[CrossRef](#)]
41. Zhang, Q.; Luan, J.; Tang, Y.; Ji, X.; Wang, H. Interfacial Design of Dendrite-Free Zinc Anodes for Aqueous Zinc-Ion Batteries. *Angew. Chem. Int. Ed.* **2020**, *59*, 13180–13191. [[CrossRef](#)] [[PubMed](#)]
42. Mitha, A.; Yazdi, A.Z.; Ahmed, M.; Chen, P. Surface Adsorption of Polyethylene Glycol to Suppress Dendrite Formation on Zinc Anodes in Rechargeable Aqueous Batteries. *ChemElectroChem* **2018**, *5*, 2409–2418. [[CrossRef](#)]
43. Luan, J.; Zhang, Q.; Yuan, H.; Sun, D.; Peng, Z.; Tang, Y.; Ji, X.; Wang, H. Plasma-Strengthened Lithiophilicity of Copper Oxide Nanosheet-Decorated Cu Foil for Stable Lithium Metal Anode. *Adv. Sci.* **2019**, *6*, 1901433. [[CrossRef](#)]
44. Zheng, J.; Zhao, Q.; Tang, T.; Yin, J.; Quilty, C.D.; Renderos, G.D.; Liu, X.; Deng, Y.; Wang, L.; Bock, D.C.; et al. Reversible epitaxial electrodeposition of metals in battery anodes. *Science* **2019**, *366*, 645–648. [[CrossRef](#)] [[PubMed](#)]
45. Wang, T.; Li, C.; Xie, X.; Lu, B.; He, Z.; Liang, S.; Zhou, J. Anode Materials for Aqueous Zinc Ion Batteries: Mechanisms, Properties, and Perspectives. *ACS Nano* **2020**, *14*, 16321–16347. [[CrossRef](#)] [[PubMed](#)]
46. Takeda, Y.; Yamamoto, O.; Imanishi, N. Lithium dendrite formation on a lithium metal anode from liquid, polymer and solid electrolytes. *Electrochemistry* **2016**, *84*, 210–218. [[CrossRef](#)]
47. Wang, D.; Zhang, W.; Zheng, W.; Cui, X.; Rojo, T.; Zhang, Q. Towards High-Safe Lithium Metal Anodes: Suppressing Lithium Dendrites via Tuning Surface Energy. *Adv. Sci.* **2017**, *4*, 1600168. [[CrossRef](#)]

48. Xu, M.; Chen, J.; Zhang, Y.; Raza, B.; Lai, C.; Wang, J. Electrolyte design strategies towards long-term Zn metal anode for rechargeable batteries. *J. Energy Chem.* **2022**, *73*, 575–587. [CrossRef]
49. Yang, J.; Yin, B.; Sun, Y.; Pan, H.; Sun, W.; Jia, B.; Zhang, S.; Ma, T. Zinc Anode for Mild Aqueous Zinc-Ion Batteries: Challenges, Strategies, and Perspectives. *Nano-Micro Lett.* **2022**, *14*, 32–78. [CrossRef]
50. Cai, Z.; Ou, Y.; Wang, J.; Xiao, R.; Fu, L.; Yuan, Z.; Zhan, R.; Sun, Y. Chemically resistant Cu-Zn/Zn composite anode for long cycling aqueous batteries. *Energy Storage Mater.* **2020**, *27*, 205–211. [CrossRef]
51. Lei, L.; Sun, Y.; Wang, X.; Jiang, Y.; Li, J. Strategies to Enhance Corrosion Resistance of Zn Electrodes for Next Generation Batteries. *Front. Mater.* **2020**, *7*, 96. [CrossRef]
52. Zhang, T.; Tang, Y.; Guo, S.; Cao, X.; Pan, A.; Fang, G.; Zhou, J.; Liang, S. Fundamentals and perspectives in developing zinc-ion battery electrolytes: A comprehensive review. *Energy Environ. Sci.* **2020**, *13*, 4625–4665. [CrossRef]
53. Geng, Y.; Miao, L.; Yan, Z.; Xin, W.; Zhang, L.; Peng, H.; Li, J.; Zhu, Z. Super-zincophilic additive induced interphase modulation enables long-life Zn anodes at high current density and areal capacity. *J. Mater. Chem. A* **2022**, *10*, 10132–10138. [CrossRef]
54. Wang, L.; Yan, S.; Quilty, C.D.; Kuang, J.; Dunkin, M.R.; Ehrlich, S.N.; Ma, L.; Takeuchi, K.J.; Takeuchi, E.S.; Marschilok, A.C. Achieving Stable Molybdenum Oxide Cathodes for Aqueous Zinc-Ion Batteries in Water-in-Salt Electrolyte. *Adv. Mater. Interfaces* **2021**, *8*, 2002080. [CrossRef]
55. Zhang, H.; Liu, X.; Qin, B.; Passerini, S. Electrochemical intercalation of anions in graphite for high-voltage aqueous zinc battery. *J. Power Sources* **2020**, *449*, 227594. [CrossRef]
56. Olbasa, B.W.; Fenta, F.W.; Chiu, S.-F.; Tsai, M.-C.; Huang, C.-J.; Jote, B.A.; Beyene, T.T.; Liao, Y.-F.; Wang, C.-H.; Su, W.-N.; et al. High-Rate and Long-Cycle Stability with a Dendrite-Free Zinc Anode in an Aqueous Zn-Ion Battery Using Concentrated Electrolytes. *ACS Appl. Energy Mater.* **2020**, *3*, 4499–4508. [CrossRef]
57. Qiu, M.; Sun, P.; Qin, A.; Cui, G.; Mai, W. Metal-coordination chemistry guiding preferred crystallographic orientation for reversible zinc anode. *Energy Storage Mater.* **2022**, *49*, 463–470. [CrossRef]
58. Han, D.; Wang, Z.; Lu, H.; Li, H.; Cui, C.; Zhang, Z.; Sun, R.; Geng, C.; Liang, Q.; Guo, X.; et al. A Self-Regulated Interface toward Highly Reversible Aqueous Zinc Batteries. *Adv. Energy Mater.* **2022**, *12*, 2102982. [CrossRef]
59. Zhu, J.; Deng, W.; Yang, N.; Xu, X.; Huang, C.; Zhou, Y.; Zhang, M.; Yuan, X.; Hu, J.; Li, C.; et al. Biomolecular Regulation of Zinc Deposition to Achieve Ultra-Long Life and High-Rate Zn Metal Anodes. *Small* **2022**, *18*, 2202509. [CrossRef]
60. Chang, G.; Liu, S.; Fu, Y.; Hao, X.; Jin, W.; Ji, X.; Hu, J. Inhibition Role of Trace Metal Ion Additives on Zinc Dendrites during Plating and Stripping Processes. *Adv. Mater. Interfaces* **2019**, *6*, 1901358. [CrossRef]
61. Wang, P.; Xie, X.; Xing, Z.; Chen, X.; Fang, G.; Lu, B.; Zhou, J.; Liang, S.; Fan, H.J. Mechanistic Insights of Mg²⁺-Electrolyte Additive for High-Energy and Long-Life Zinc-Ion Hybrid Capacitors. *Adv. Energy Mater.* **2021**, *11*, 2101158. [CrossRef]
62. Zhao, R.; Wang, H.; Du, H.; Yang, Y.; Gao, Z.; Qie, L.; Huang, Y. Lanthanum nitrate as aqueous electrolyte additive for favourable zinc metal electrodeposition. *Nat. Commun.* **2022**, *13*, 3252. [CrossRef] [PubMed]
63. Liu, Y.; Shi, Q.; Wu, Y.; Wang, Q.; Huang, J.; Chen, P. Highly efficient dendrite suppressor and corrosion inhibitor based on gelatin/Mn²⁺ Co-additives for aqueous rechargeable zinc-manganese dioxide battery. *Chem. Eng. J.* **2021**, *407*, 127189. [CrossRef]
64. Nie, X.; Miao, L.; Yuan, W.; Ma, G.; Di, S.; Wang, Y.; Shen, S.; Zhang, N. Cholinium Cations Enable Highly Compact and Dendrite-Free Zn Metal Anodes in Aqueous Electrolytes. *Adv. Funct. Mater.* **2022**, *32*, 2203905. [CrossRef]
65. Yao, R.; Qian, L.; Sui, Y.; Zhao, G.; Guo, R.; Hu, S.; Liu, P.; Zhu, H.; Wang, F.; Zhi, C.; et al. A Versatile Cation Additive Enabled Highly Reversible Zinc Metal Anode. *Adv. Energy Mater.* **2022**, *12*, 2102780. [CrossRef]
66. Guo, X.; Zhang, Z.; Li, J.; Luo, N.; Chai, G.-L.; Miller, T.S.; Lai, F.; Shearing, P.; Brett, D.J.L.; Han, D.; et al. Alleviation of Dendrite Formation on Zinc Anodes via Electrolyte Additives. *ACS Energy Lett.* **2021**, *6*, 395–403. [CrossRef]
67. Xu, Y.; Zhu, J.; Feng, J.; Wang, Y.; Wu, X.; Ma, P.; Zhang, X.; Wang, G.; Yan, X.J.E.S.M. A rechargeable aqueous zinc/sodium manganese oxides battery with robust performance enabled by Na₂SO₄ electrolyte additive. *Energy Storage Mater.* **2021**, *38*, 299–308. [CrossRef]
68. Zhou, X.; Ma, K.; Zhang, Q.; Yang, G.; Wang, C. Highly stable aqueous zinc-ion batteries enabled by suppressing the dendrite and by-product formation in multifunctional Al³⁺ electrolyte additive. *Nano Res.* **2022**, *15*, 8039–8047. [CrossRef]
69. Liu, S.; Shang, W.; Yang, Y.; Kang, D.; Li, C.; Sun, B.; Kang, L.; Yun, S.; Jiang, F. Effects of I₃⁻ Electrolyte Additive on the Electrochemical Performance of Zn Anodes and Zn/MnO₂ Batteries. *Batter. Supercaps* **2022**, *5*, e202100221. [CrossRef]
70. Otani, T.; Fukunaka, Y.; Homma, T. Effect of lead and tin additives on surface morphology evolution of electrodeposited zinc. *Electrochim. Acta* **2017**, *242*, 364–372. [CrossRef]
71. Luo, M.; Zhang, R.; Gong, Y.; Wang, M.; Chen, Y.; Chu, M.; Chen, L. Effects of doping Al on the structure and electrochemical performances of Li[Li_{0.2}Mn_{0.54}Ni_{0.13}Co_{0.13}]O₂ cathode materials. *Ionics* **2018**, *24*, 967–976. [CrossRef]
72. Zhou, K.; Xie, Q.; Li, B.; Manthiram, A. An in-depth understanding of the effect of aluminum doping in high-nickel cathodes for lithium-ion batteries. *Energy Storage Mater.* **2021**, *34*, 229–240. [CrossRef]
73. Xu, W.; Zheng, Y.; Cheng, Y.; Qi, R.; Peng, H.; Lin, H.; Huang, R. Understanding the Effect of Al Doping on the Electrochemical Performance Improvement of the LiMn₂O₄ Cathode Material. *ACS Appl. Mater. Interfaces* **2021**, *13*, 45446–45454. [CrossRef] [PubMed]
74. Han, L.; Huang, H.; Li, J.; Zhang, X.; Yang, Z.; Xu, M.; Pan, L. A novel redox bromide-ion additive hydrogel electrolyte for flexible Zn-ion hybrid supercapacitors with boosted energy density and controllable zinc deposition. *J. Mater. Chem. A* **2020**, *8*, 15042–15050. [CrossRef]

75. Wang, S.; Li, T.; Yin, Y.; Chang, N.; Zhang, H.; Li, X. High-energy-density aqueous zinc-based hybrid supercapacitor-battery with uniform zinc deposition achieved by multifunctional decoupled additive. *Nano Energy* **2022**, *96*, 107120. [\[CrossRef\]](#)
76. Chen, C.; Li, Z.; Xu, Y.; An, Y.; Wu, L.; Sun, Y.; Liao, H.; Zheng, K.; Zhang, X. High-Energy Density Aqueous Zinc–Iodine Batteries with Ultra-long Cycle Life Enabled by the ZnI_2 Additive. *ACS Sustain. Chem. Eng.* **2021**, *9*, 13268–13276. [\[CrossRef\]](#)
77. Bayaguud, A.; Luo, X.; Fu, Y.; Zhu, C. Cationic Surfactant-Type Electrolyte Additive Enables Three-Dimensional Dendrite-Free Zinc Anode for Stable Zinc-Ion Batteries. *ACS Energy Lett.* **2020**, *5*, 3012–3020. [\[CrossRef\]](#)
78. Zhao, X.; Zhang, X.; Dong, N.; Yan, M.; Zhang, F.; Mochizuki, K.; Pan, H. Advanced Buffering Acidic Aqueous Electrolytes for Ultra-Long Life Aqueous Zinc-Ion Batteries. *Small* **2022**, *18*, 2200742. [\[CrossRef\]](#)
79. Yang, X.; Liu, S.; Tang, J.; Chang, G.; Fu, Y.; Jin, W.; Ji, X.; Hu, J. Effective inhibition of zinc dendrites during electrodeposition using thiourea derivatives as additives. *J. Mater. Sci.* **2019**, *54*, 3536–3546. [\[CrossRef\]](#)
80. Banik, S.J.; Akolkar, R. Suppressing Dendritic Growth during Alkaline Zinc Electrodeposition using Polyethylenimine Additive. *Electrochim. Acta* **2015**, *179*, 475–481. [\[CrossRef\]](#)
81. Dong, Y.; Miao, L.; Ma, G.; Di, S.; Wang, Y.; Wang, L.; Xu, J.; Zhang, N. Non-concentrated aqueous electrolytes with organic solvent additives for stable zinc batteries. *Chem. Sci.* **2021**, *12*, 5843–5852. [\[CrossRef\]](#) [\[PubMed\]](#)
82. Miao, L.; Wang, R.; Di, S.; Qian, Z.; Zhang, L.; Xin, W.; Liu, M.; Zhu, Z.; Chu, S.; Du, Y.; et al. Aqueous Electrolytes with Hydrophobic Organic Cosolvents for Stabilizing Zinc Metal Anodes. *ACS Nano* **2022**, *16*, 9667–9678. [\[CrossRef\]](#) [\[PubMed\]](#)
83. Lin, C.; Yang, X.; Xiong, P.; Lin, H.; He, L.; Yao, Q.; Wei, M.; Qian, Q.; Chen, Q.; Zeng, L. High-Rate, Large Capacity, and Long Life Dendrite-Free Zn Metal Anode Enabled by Trifunctional Electrolyte Additive with a Wide Temperature Range. *Adv. Sci.* **2022**, *9*, 2201433. [\[CrossRef\]](#) [\[PubMed\]](#)
84. Wijitrat, A.; Qin, J.; Kasemchainan, J.; Tantavichet, N. Ethylene carbonate as an organic electrolyte additive for high-performance aqueous rechargeable zinc-ion batteries. *J. Ind. Eng. Chem.* **2022**, *112*, 96–105. [\[CrossRef\]](#)
85. Miao, Z.; Liu, Q.; Wei, W.; Zhao, X.; Du, M.; Li, H.; Zhang, F.; Hao, M.; Cui, Z.; Sang, Y.; et al. Unveiling unique steric effect of threonine additive for highly reversible Zn anode. *Nano Energy* **2022**, *97*, 107145. [\[CrossRef\]](#)
86. Meng, Q.; Zhao, R.; Cao, P.; Bai, Q.; Tang, J.; Liu, G.; Zhou, X.; Yang, J. Stabilization of Zn anode via a multifunctional cysteine additive. *Chem. Eng. J.* **2022**, *447*, 137471. [\[CrossRef\]](#)
87. Shi, J.; Xia, K.; Liu, L.; Liu, C.; Zhang, Q.; Li, L.; Zhou, X.; Liang, J.; Tao, Z. Ultrahigh coulombic efficiency and long-life aqueous Zn anodes enabled by electrolyte additive of acetonitrile. *Electrochim. Acta* **2020**, *358*, 136937. [\[CrossRef\]](#)
88. Naveed, A.; Yang, H.; Shao, Y.; Yang, J.; Yanna, N.; Liu, J.; Shi, S.; Zhang, L.; Ye, A.; He, B.; et al. A Highly Reversible Zn Anode with Intrinsically Safe Organic Electrolyte for Long-Cycle-Life Batteries. *Adv. Mater.* **2019**, *31*, 1900668. [\[CrossRef\]](#)
89. Zhou, M.; Chen, H.; Chen, Z.; Hu, Z.; Wang, N.; Jin, Y.; Yu, X.; Meng, H. Nonionic Surfactant Coconut Diethanol Amide Inhibits the Growth of Zinc Dendrites for More Stable Zinc-Ion Batteries. *ACS Appl. Energy Mater.* **2022**, *5*, 7590–7599. [\[CrossRef\]](#)
90. Xia, S.; Lopez, J.; Liang, C.; Zhang, Z.; Bao, Z.; Cui, Y.; Liu, W. High-Rate and Large-Capacity Lithium Metal Anode Enabled by Volume Conformal and Self-Healable Composite Polymer Electrolyte. *Adv. Sci.* **2019**, *6*, 1802353. [\[CrossRef\]](#)
91. Li, C.; Shyamsunder, A.; Hoane, A.G.; Long, D.M.; Kwok, C.Y.; Kotula, P.G.; Zavadil, K.R.; Gewirth, A.A.; Nazar, L.F. Highly reversible Zn anode with a practical areal capacity enabled by a sustainable electrolyte and superacid interfacial chemistry. *Joule* **2022**, *6*, 1103–1120. [\[CrossRef\]](#)
92. Chen, A.; Zhao, C.; Guo, Z.; Lu, X.; Zhang, J.; Liu, N.; Zhang, Y.; Zhang, N. Stabilized Zn Anode Based on SO_4^{2-} Trapping Ability and High Hydrogen Evolution Barrier. *Adv. Funct. Mater.* **2022**, *32*, 2203595. [\[CrossRef\]](#)
93. Huang, C.; Zhao, X.; Liu, S.; Hao, Y.; Tang, Q.; Hu, A.; Liu, Z.; Chen, X. Stabilizing Zinc Anodes by Regulating the Electrical Double Layer with Saccharin Anions. *Adv. Mater.* **2021**, *33*, 2100445. [\[CrossRef\]](#) [\[PubMed\]](#)
94. Bani Hashemi, A.; Kasiri, G.; La Mantia, F. The effect of polyethylenimine as an electrolyte additive on zinc electrodeposition mechanism in aqueous zinc-ion batteries. *Electrochim. Acta* **2017**, *258*, 703–708. [\[CrossRef\]](#)
95. Zhou, T.; Mu, Y.; Chen, L.; Li, D.; Liu, W.; Yang, C.; Zhang, S.; Wang, Q.; Jiang, P.; Ge, G.; et al. Toward stable zinc aqueous rechargeable batteries by anode morphology modulation via polyaspartic acid additive. *Energy Storage Mater.* **2022**, *45*, 777–785. [\[CrossRef\]](#)
96. Feng, D.; Cao, F.; Hou, L.; Li, T.; Jiao, Y.; Wu, P. Immunizing Aqueous Zn Batteries against Dendrite Formation and Side Reactions at Various Temperatures via Electrolyte Additives. *Small* **2021**, *17*, 2103195. [\[CrossRef\]](#)
97. Cao, Z.; Zhu, X.; Gao, S.; Xu, D.; Wang, Z.; Ye, Z.; Wang, L.; Chen, B.; Li, L.; Ye, M.; et al. Ultrastable Zinc Anode by Simultaneously Manipulating Solvation Sheath and Inducing Oriented Deposition with PEG Stability Promoter. *Small* **2022**, *18*, 2103345. [\[CrossRef\]](#)
98. Shang, Y.; Kumar, P.; Musso, T.; Mittal, U.; Du, Q.; Liang, X.; Kundu, D. Long-Life Zn Anode Enabled by Low Volume Concentration of a Benign Electrolyte Additive. *Adv. Funct. Mater.* **2022**, *32*, 2200606. [\[CrossRef\]](#)
99. Zhao, K.; Fan, G.; Liu, J.; Liu, F.; Li, J.; Zhou, X.; Ni, Y.; Yu, M.; Zhang, Y.-M.; Su, H.; et al. Boosting the Kinetics and Stability of Zn Anodes in Aqueous Electrolytes with Supramolecular Cyclodextrin Additives. *J. Am. Chem. Soc.* **2022**, *144*, 11129–11137. [\[CrossRef\]](#)
100. Lin, X.-S.; Wang, Z.-R.; Ge, L.-H.; Xu, J.-W.; Ma, W.-Q.; Ren, M.-M.; Liu, W.-L.; Yao, J.-S.; Zhang, C.-B. Electrolyte Modification for Long-Life Zn Ion Batteries: Achieved by Methanol Additive. *ChemElectroChem* **2022**, *9*, e202101724. [\[CrossRef\]](#)

101. Ma, L.; Vatamanu, J.; Hahn, N.T.; Pollard, T.P.; Borodin, O.; Petkov, V.; Schroeder, M.A.; Ren, Y.; Ding, M.S.; Luo, C.; et al. Highly reversible Zn metal anode enabled by sustainable hydroxyl chemistry. *Proc. Natl. Acad. Sci. USA* **2022**, *119*, e2121138119. [[CrossRef](#)] [[PubMed](#)]
102. Ji, H.; Han, Z.; Lin, Y.; Yu, B.; Wu, D.; Zhao, L.; Wang, M.; Chen, J.; Ma, Z.; Guo, B.; et al. Stabilizing zinc anode for high-performance aqueous zinc ion batteries via employing a novel inositol additive. *J. Alloy Compd.* **2022**, *914*, 165231. [[CrossRef](#)]
103. Wu, F.; Chen, Y.; Chen, Y.; Yin, R.; Feng, Y.; Zheng, D.; Xu, X.; Shi, W.; Liu, W.; Cao, X. Achieving Highly Reversible Zinc Anodes via N,N-Dimethylacetamide Enabled Zn-Ion Solvation Regulation. *Small* **2022**, *18*, 2202363. [[CrossRef](#)]
104. Sun, K.E.K.; Hoang, T.K.A.; Doan, T.N.L.; Yu, Y.; Chen, P. Highly Sustainable Zinc Anodes for a Rechargeable Hybrid Aqueous Battery. *Chem. Eur. J.* **2018**, *24*, 1667–1673. [[CrossRef](#)]
105. Lee, C.W.; Sathiyanarayanan, K.; Eom, S.W.; Kim, H.S.; Yun, M.S. Novel electrochemical behavior of zinc anodes in zinc/air batteries in the presence of additives. *J. Power Sources* **2006**, *159*, 1474–1477. [[CrossRef](#)]
106. Hamilton, S.T.; Feric, T.G.; Gladysiak, A.; Cantillo, N.M.; Zawodzinski, T.A.; Park, A.-H.A. Mechanistic Study of Controlled Zinc Electrodeposition Behaviors Facilitated by Nanoscale Electrolyte Additives at the Electrode Interface. *ACS Appl. Mater. Interfaces* **2022**, *14*, 22016–22029. [[CrossRef](#)]
107. Huang, C.; Zhao, X.; Hao, Y.; Yang, Y.; Qian, Y.; Chang, G.; Zhang, Y.; Tang, Q.; Hu, A.; Chen, X. Self-Healing SeO₂ Additives Enable Zinc Metal Reversibility in Aqueous ZnSO₄ Electrolytes. *Adv. Funct. Mater.* **2022**, *32*, 2112091. [[CrossRef](#)]
108. Zhang, Y.; Huang, Z.; Wu, K.; Yu, F.; Zhu, M.; Wang, G.; Xu, G.; Wu, M.; Liu, H.-K.; Dou, S.-X.; et al. 2D anionic nanosheet additive for stable Zn metal anodes in aqueous electrolyte. *Chem. Eng. J.* **2022**, *430*, 133042. [[CrossRef](#)]
109. Sun, C.; Wu, C.; Gu, X.; Wang, C.; Wang, Q. Interface Engineering via Ti₃C₂T_x MXene Electrolyte Additive toward Dendrite-Free Zinc Deposition. *Nano-Micro Lett.* **2021**, *13*, 89. [[CrossRef](#)]
110. Zhang, H.; Guo, R.; Li, S.; Liu, C.; Li, H.; Zou, G.; Hu, J.; Hou, H.; Ji, X. Graphene quantum dots enable dendrite-free zinc ion battery. *Nano Energy* **2022**, *92*, 106752. [[CrossRef](#)]
111. Naguib, M.; Kurtoglu, M.; Presser, V.; Lu, J.; Niu, J.; Heon, M.; Hultman, L.; Gogotsi, Y.; Barsoum, M.W. Two-Dimensional Nanocrystals Produced by Exfoliation of Ti₃AlC₂. *Adv. Mater.* **2011**, *23*, 4248–4253. [[CrossRef](#)] [[PubMed](#)]
112. Tang, X.; Zhou, D.; Li, P.; Guo, X.; Sun, B.; Liu, H.; Yan, K.; Gogotsi, Y.; Wang, G. MXene-Based Dendrite-Free Potassium Metal Batteries. *Adv. Mater.* **2020**, *32*, 1906739. [[CrossRef](#)] [[PubMed](#)]
113. Sun, C.; Shi, X.; Zhang, Y.; Liang, J.; Qu, J.; Lai, C. Ti₃C₂T_x MXene Interface Layer Driving Ultra-Stable Lithium-Iodine Batteries with Both High Iodine Content and Mass Loading. *ACS Nano* **2020**, *14*, 1176–1184. [[CrossRef](#)] [[PubMed](#)]
114. Abdulla, J.; Cao, J.; Zhang, D.; Zhang, X.; Sriprachuabwong, C.; Kheawhom, S.; Wangyao, P.; Qin, J. Elimination of Zinc Dendrites by Graphene Oxide Electrolyte Additive for Zinc-Ion Batteries. *ACS Appl. Energy Mater.* **2021**, *4*, 4602–4609. [[CrossRef](#)]